EXPLORATION OF NANO-STRUCTURE MELDING VIA COMPUTER SIMULATION

SENIOR HONORS THESIS

Presented in Partial Fulfillment of the Requirements for Distinction in the Chemical Engineering Bachelors of Science Program

By

Daniel Griffin

Undergraduate Program in Chemical and Biomolecular Engineering

The Ohio State University

2011

Committee:

Dr. Isamu Kusaka, Advisor

Dr. David L. Tomasko

ABSTRACT

Motivated by the desire to have analytic capabilities at the point of care, small, portable devices, such as “Lab on a Chip” (LOC), are being developed; however, in order to commercialize many of these newly developed tools, cost effective nanostructure processing techniques must be introduced. It has been suggested that some processing complications could be avoided if separately formed structural fragments could be combined to form the more complicated desired nanostructure. The goal of this research project is to explore the possibility of using a melding process in the production of LOC and like technologies. However, as the designed structural features of these chips are on the order of nanometers, it is very difficult and expensive to do a *lab* study of the related phenomenon at the required scale. Fortunately, computer simulations provide an increasingly fast and accurate alternative to physical experiments.

High-pressure CO_2 has the ability to widen the interfacial region and make the surface of plastic [polymer] structures rubbery at temperatures much lower than the Glass Transition Temperature (T_g). As a result, CO_2 may be used to facilitate the mentioned melding process. This project is therefore primarily concerned with using computer simulation to examine the effects of CO_2 on the T_g of plastic. Specifically, a FORTRAN code developed by Dr. Isamu Kusaka is used to perform molecular-level simulations that have been designed to elicit important characteristics of the phenomenon of particular interest, glass transition.

The Glass Transition Temperature of a pure plastic may be found using a Monte Carlo cooling simulation in which volume is recorded against temperature. Examining the glass transition of a plastic subject to CO_2, however, proves to be more difficult. As a result, this project examines a possible alternative method for extracting the T_g of a multispecies system via a mobility indicator, D_{MC}.

To extend this project and fully explore the possibility of a CO_2 assisted nanostructure-melding process, methods for extracting the T_g of a plastic subject to CO_2 must be refined. Furthermore, techniques to examine the interfacial region and simulate polymer-polymer melding must be established.

ACKNOWLEDGMENTS

First I would like to thank Dr. Isamu Kusaka. As a teacher Dr. Kusaka has been inspirational and, in a true testament to his kindness, was willing to create a research position for me, find funding for me, and, in general, go out of his way to make my last few years at Ohio State enjoyable, informative and productive. I would also like to thank Dr. David L. Tomasko, Dr. Manish Taljera, Adam Burley and Lu Feng. Although at times very busy, Dr. Tomasko was always willing to sit through my research presentations, offer suggestions and encourage me. The conversations I had with Dr. Taljera while he was still at Ohio State were invaluable and helped guide my research. Adam Burley patiently showed me the ropes – from helping me set up for presentations to advising me on being a TA. Also, thanks to Clay Housholder for all of the help in organizing and composing this thesis.

Finally, I would like to thank my family; my parents David and Laurie, and my brothers, Ryan and Mike. In a few short sentences it's impossible to capture how much my family has done to make my life easy and enjoyable – I would simply like to say thank you.

VITA

July 13, 1987……Born – Dayton, OH

September, 2006 – June, 2011……B.S., Chemical Engineering
The Ohio State University

FIELDS OF STUDY

Major Field: Chemical and Biomolecular Engineering

Minor Field: Nuclear Engineering

Contents

Tables: viii
Figures: viii
Introduction 1
Background 2
Contents of This Thesis 4
1. Simulation 6
Simulating Molecular Motion/Rearrangement 8
monte carlo simulation. 8
molecular dynamics simulation 10
Temperature, Pressure, Volume and Boundary Condition in Simulation 10
temperature. 10
pressure and volume. 11
boundary condition in simulation. 12
Reduced Critical Temperature and Pressure and Molecule Parameters 13
2. Simulating a Polymer 16
Simulated Polymer Parameters 16
Obtaining the T_g of a Pure Polymer Via MC Simulation 18
statistical analysis of the pure polymer volume curve. 20
3. Introducing CO_2 27
Two-box Simulation 27
"Parameterizing" CO_2 27
cross interactions. 28
Initial Two-box Cooling Simulation 30
Changing the CO_2 Parameters 31
4. Pure polymer Glass Transition Temperatures at 10 MPa and 15MPa 33
5. Finding the T_g of a Polymer with Dissolved CO_2 36
Two-box Simulation with New CO_2 Parameters 36

Lower Bound on Simulation Box Size 42
Re-Examination of the Effect of CO2 on the Polymer Glass Transition Temperature 45
6. Diffusion Coefficient and Glass Transition Temperature 52
Finding the Diffusion Coefficient from a MC CS 53
Diffusion Coefficient of the Polymer Subject to CO_2 55
Pure Polymer Diffusion Coefficient 59
7. Work in Progress and Suggested Further Work 63
Diffusion Coefficient – Further Work 63
glass region. 63
revised measure of diffusion. 63
Volume Deviation 65
Heating vs. Cooling MC Simulation 67
Conclusion 68
References 70
APPENDIX 71
Appendix A 72
statistical analysis. 72
Appendix B 74
slope of log plot vs. temperature. 74
Appendix C 75
cooling vs. heating MC CS. 75

Tables:

Table 1: Tg and Glass Transition Range for the pure CS polymer at different pressures 35

Figures:

Figure 1: Schematic of film adhesion attempts when the structures are completely solid (i.), when the entire structures are rubbery (ii.), and when just the edges of the structures are rubbery (iii.). 2
Figure 2: Effect if film thickness and CO2 on the interfacial width at 10 MPa and 323K (Taljera, 2010) 3
Figure 3: Arbitrary depiction of CO2 dissolved at higher concentrations near the polymer surface, depressing the Glass Transition Temperature in that region. 4
Figure 4: Cartoon of simulation containing five particles 6
Figure 5: Interaction energy of argon dimer. Empirical results taken from R. A. Aziz, J. Chem. Phys., vol. 99, 4518 (1993), Lennard-Jones fitted to the empirical results (Poszwa, 2005) (Aziz, 1993). 6
Figure 6: Simulation of polymers 8
Figure 7: MC simulation step 1 9
Figure 8: MC simulation steps 2 and 3 10
Figure 9: Qualitative depiction of the equilibrium that must exist between the number of molecules, temperature [although this is difficult to illustrate here], volume and pressure. At the equilibrated volume the pressures must be equal. 11
Figure 10: Illustration of volume change 12
Figure 11: Classic Depiction of a periodic boundary condition in 2D 13
Figure 12: Volume of pure polymer vs. temperature at atmospheric pressure 19
Figure 13: Dv/dT vs. temperature 19
Figure 14: Plotting dV/dT vs. temperature suggests a glass transition region of ~ 140 K to 190 K 20
Figure 15: Statistical analysis of the volume vs. temperature data obtained for the pure polymer at atmospheric pressure 25
Figure 16: Plotting the volume vs. temperature obtained via a MC cooling simulation indicates a Tg of ~ 170K at atmospheric pressure. 26
Figure 17: two-box simulation (polymer segments - red; CO_2 molecules - blue) 27
Figure 18: Depiction of cross interactions in mixtures 28
Figure 19: Lorentz-Berthelot mixing rules 28

Figure 20: Finding the cross interaction epsilon adjustment parameter 29
Figure 21: Solubility comparison between experimental data and results from a two-box simulation. (Talreja, 2010) 30
Figure 22: Volume vs. temperature for the pure CS polymer, at 10 MPa. Tg ~ 183 K 33
Figure 23: DV/dT vs. temperature for the pure CS polymer at 10 MPa. Glass Transition range ~ 160-200K. 33
Figure 24: Volume vs. temperature for the pure CS polymer, at 15 MPa. Tg ~ 183 .. 34
Figure 25: DV/dT vs. temperature for the pure CS polymer at 15 MPa. Glass Transition range ~ 170-210K. 34
Figure 26: Gives the mole fraction of CO2 in the CO2-polymer box. From the 2-box cooling simulation, using the new CO2 parameters run at 15 MPa 37
Figure 27: Gives the number density (total number of CO2 molecules + polymer segments per volume) in the CO2-polymer box. From the 2-box cooling simulation, using the new CO2 parameters run at 15 MPa 37
Figure 28: Gives the CO2 number density (number of CO2 molecules per volume) in the CO2-polymer box. From the 2-box cooling simulation, using the new CO2 parameters run at 15 MPa 37
Figure 29: Gives the volume of the CO2-polymer box. From the 2-box cooling simulation, using the new CO2 parameters run at 15 MPa 38
Figure 30: Gives the mole fraction of CO2 in the CO2-polymer box. From the 2-box cooling simulation, using the new CO2 parameters run at 10 38
Figure 31: Gives the number density (total number of CO2 molecules + polymer segments per volume) in the CO2-polymer box. From the 2-box cooling simulation, using the new CO2 parameters run at 10 MPa 38
Figure 32: Gives the CO2 number density (number of CO2 molecules per volume) in the CO2-polymer box. From the 2-box cooling simulation, using the new CO2 parameters run at 10 MPa 39
Figure 33: Gives the volume of the CO2-polymer box. From the 2-box cooling simulation, using the new CO2 parameters run at 10 MPa 39
Figure 34: Shows the CO2 density in the CO2 only box at 10 MPa. 40
Figure 35: Shows the CO2 density in the CO2 only box at 15 MPa. Notice the odd densities for temperatures lower than 180 K 40
Figure 36: Shows the pressure in the pure CO_2 box (P* that corresponds to 15 MPa is .1507461) 41
Figure 37: Shows the pressure in the pure CO_2 box (P* that corresponds to 10 MPa is .1004974) 41
Figure 38: Cartoon depicting the effect of the box size restriction 42
Figure 39: Shows the number density in the CO_2-only box after increasing the number of CO2 molecules to avoid the minimum volume issue 43

Figure 40: Shows the calculated pressure in the CO2-only box after increasing the number of CO2 molecules to avoid the minimum volume issue. 43
Figure 41: Shows the number density in the CO_2-only box after increasing the number of CO_2 molecules to avoid the minimum volume issue 44
Figure 42: Shows the calculated pressure in the CO_2-only box after increasing the number of CO_2 molecules to avoid the minimum volume issue. 44
Figure 43: Gives the mole fraction of CO2 in the CO2-polymer box. From the 2-box cooling simulation, using the new CO2 parameters run at 10 MPa 45
Figure 44: Gives the number density (total number of CO2 molecules + polymer segments per volume) in the CO2-polymer box. From the 2-box cooling simulation, using the new CO2 parameters run at 10 MPa 46
Figure 45: Gives the CO2 number density (number of CO2 molecules per volume) in the CO2-polymer box. From the 2-box cooling simulation, using the new CO2 parameters run at 10 MPa 46
Figure 46: Gives the volume of the CO2-polymer box. From the 2-box cooling simulation, using the new CO2 parameters run at 10 MPa 47
Figure 47: Gives the mole fraction of CO2 in the CO2-polymer box. From the 2-box cooling simulation, using the new CO2 parameters run at 15 MPa 47
Figure 48: Gives the number density (total number of CO2 molecules + polymer segments per volume) in the CO2-polymer box. From the 2-box cooling simulation, using the new CO2 parameters run at 15 MPa 48
Figure 49: Gives the CO2 number density (number of CO2 molecules per volume) in the CO2-polymer box. From the 2-box cooling simulation, using the new CO2 parameters run at 15 MPa 48
Figure 50: Gives the volume of the CO2-polymer box. From the 2-box cooling simulation, using the new CO2 parameters run at 15 MPa 49
Figure 51: Qualitative sketch of number density vs. temperature for a fixed number of CO2 molecules in the CO2-polymer box 50
Figure 52: Mean squared displacement including the initial transient portion 54
Figure 53: Shows the linear line fit to the ENTIRE data set in the steady-state diffusion region. Illustrating the error introduced by including the initial, transient, diffusion data. 54
Figure 54: $6*D_{MC}$ vs. temperature for a polymer subject to CO2 at 15 MPa 55
Figure 55: $6*D_{MC}$ vs. temperature for a polymer subject to CO2 at 5 MPa. A simulation error resulted in the loss of data at 180K. 56
Figure 56: $6*D_{MC}$ vs. temperature for a polymer subject to CO2 at 15 MPa (both simulations) 57
Figure 57: $6*D_{MC}$ vs. temperature for a polymer subject to CO2 at 5 MPa (both simulations) 57

Figure 58: 6*D_{MC} vs. temperature. Data grouped into regions characterized by slope 58
Figure 59: 6*D_{MC} vs. temperature. Data grouped into regions characterized by slope 58
Figure 60: 6*D_{MC} vs. temperature for pure polymer at 15 MPa 59
Figure 61: 6*DMC vs. temperature for a pure polymer at 15 MPa. Data categorized as belonging to a liquid, transition, or glassy state per previous cooling simulation on a pure polymer at 15 MPa. 60
Figure 62: 6*DMC vs. temperature for a pure polymer at 15 MPa. Data split at most apparent trend changes. 60
Figure 63: 6*DMC vs. temperature for a pure polymer at 15 MPa. Data broken into two regions, as indicated by a change in slope. 61
Figure 64: 6*DMC vs. temperature for a pure polymer at 15 MPa. In this graph the data is broken up into just two states characterized by slope. 61
Figure 65: 6*DMC vs. temperature for a pure polymer at 5 MPa. In this graph the data is broken up into just two states characterized by slope. Recall that diffusion data was lost at 180K – this made it difficult to calculate the slope for the surrounding temperatures. 62
Figure 66: Results of two replicate cooling simulations 66
Figure 67: Displays the slope of $\log(< (\Delta r)2 >)\ vs.\ \log(MC\ moves)$ against temperature 74
Figure 68: Gives the mole fraction of CO2 in the CO2-polymer box. From the 2-box heating simulation, using the new CO2 parameters run at 10 MPa 75
Figure 69: Gives the number density (total number of CO2 molecules + polymer segments per volume) in the CO2-polymer box. From the 2-box heating simulation, using the new CO2 parameters run at 10 MPa 75
Figure 70: Gives the CO2 number density (number of CO2 molecules per volume) in the CO2-polymer box. From the 2-box heating simulation, using the new CO2 parameters run at 10 MPa 76
Figure 71: Gives the volume of the CO2-polymer box. From the 2-box heating simulation, using the new CO2 parameters run at 10 MPa 76

Introduction

It is not unusual for doctors to have to wait for the lab analysis of a saliva, or blood sample before they can make a firm diagnosis. This is a considerable problem as necessary medical actions may not be taken immediately and time, effort and money is expended filling out forms, transferring samples to the lab, etc. This could be avoided if analytic capabilities that are normally restricted to a lab were made available at the point of care.

In an effort to make devices that will allow medical professionals to analyze samples on the spot, "Micro Total Analysis Systems" have been developed. These systems integrate one or multiple laboratory functions onto a chip only a few centimeters big. One such system is "Lab on a Chip" or LOC; in this case the chip is made out of the polymer [plastic], Polystyrene, and reagents are incorporated into nano-tubes. However, in order to commercialize LOC, cost effective nano-scale processing techniques must be introduced.

The techniques currently used to produce nano-tubes in LOC tend to be expensive and use chemical processes that can complicate the subsequent use of the resulting product. Some of these complications could be avoided if nano-tubes could be fabricated via a melding process, in which a nano-channel containing structure and cap [formed separately] are melded together. However, capping nano-channels using a melding process is not trivial. If the channel-containing structure and cap come together in their already formed solid states, they will not meld together (Figure 1-i). If the temperature is then raised, both structures will become rubbery throughout and melding will occur, however, the structures will also deform and the nano-channels will flatten (Figure 1-ii); thus leading to a loss of functionality. Therefore, a process in which the polymer structure and cap are made rubbery or liquid like *only at the surface* must be used. (Figure 1-iii).

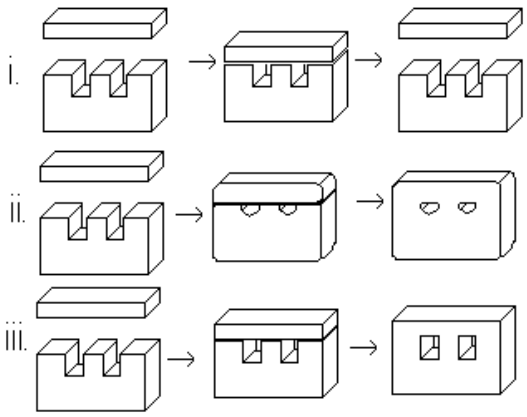

Figure 1: Schematic of film adhesion attempts when the structures are completely solid (i.), when the entire structures are rubbery (ii.), and when just the edges of the structures are rubbery (iii.).

This research project is concerned with examining the phenomena surrounding the process of melding together separately formed polymer nanostructures.

Background

In their solid state, most polymers exist as glasses. Vitrification, or the transition from liquid to glass, occurs when a glass-forming liquid [e.g. the polymer, polystyrene] has been cooled sufficiently fast to a sufficiently low temperature – not allowing enough time at each temperature for the molecules to rearrange in the lowest free energy [equilibrium] configuration. In effect, a hard substance that does not have a regular lattice configuration will form. Substances in this state are said to be in a glassy state. The temperature at which a substance undergoes a transition from liquid to glass is known as the Glass Transition Temperature (T_g). The T_g of a substance is a function of pressure, rate of cooling, and chemical makeup of that substance. Also, if the substance is not homogeneous, T_g must be regarded as a function of position.

Physical properties near the surface of polymer thin films are significantly different from bulk phase properties (Taljera, 2010). The reason properties deviate near the surface is still somewhat unclear, although this is generally considered the

result of a combination of effects stemming from increased free volume, enhanced mobility, preferential polymer chain alignment, decreased confinement and decreased density near the surface. In this near-surface area, known as the interfacial region, a reduction in the T_g is observed. This is crucial to melding polymer nanostructures.

It has been demonstrated that the surface effects observed in polymer thin films are enhanced by CO_2 (Yang, Liu, Xie, Lee, & Tomasko, 2007). In the presence of CO_2 yang et al observed a widening of the interfacial region from 2.5 nm to 10 nm. As shown in the following figure (Figure 2), simulations performed by Dr. Manish Talerja also suggest a widening of the interfacial region in the presence of CO_2.

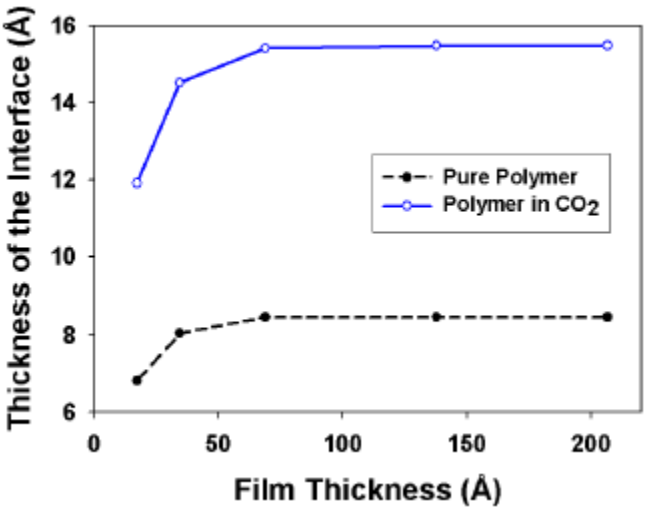

Figure 2: Effect if film thickness and CO2 on the interfacial width at 10 MPa and 323K (Taljera, 2010)

This has led to the suggestion that CO_2 may be used to facilitate the aforementioned adhesion process. The idea is, CO_2 will dissolve in plastic structures with a higher localized concentration near the solid-gas interface, disrupting the configuration as well as polymer-polymer intermolecular interactions and widening the interfacial region – again, within this region, the Glass Transition Temperature is lower than that of the bulk polymer (Figure 3 gives a rough visual). Under the right conditions, this may cause the surface to be rubbery while the rest of the structure remains rigid.

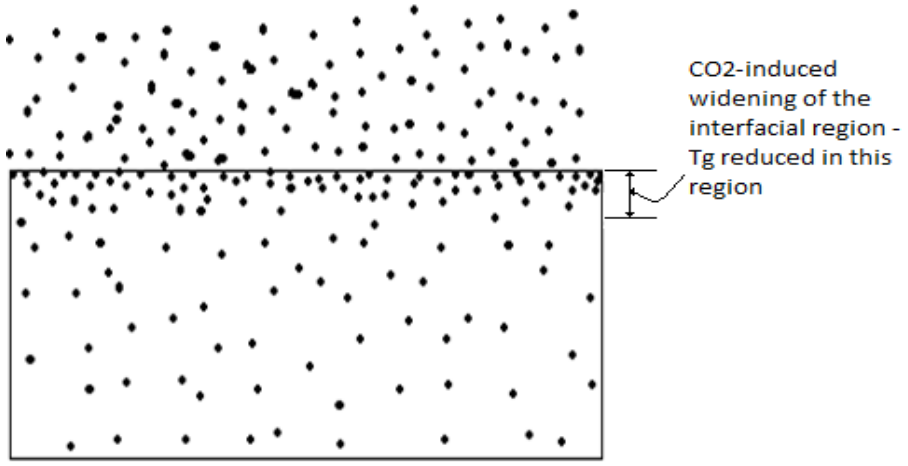

Figure 3: Arbitrary depiction of CO2 dissolved at higher concentrations near the polymer surface, depressing the Glass Transition Temperature in this region.

Medium for Exploration

As structural features in these chips are on the order of nano-meters, it is very difficult and expensive to do a *lab* study of the related phenomenon. Furthermore, glass transition and interfacial dynamics are complicated to the extent that theoretical predictions of the effects of CO_2 on T_g and properties of the polymer interface are lacking. Fortunately, computer simulations provide an increasingly fast and accurate alternative to physical experiments. In this project a FORTRAN code developed by Dr. Isamu Kusaka is used to perform molecular level simulations designed to elicit the effects of CO_2 on the glass transition of a plastic.

Contents of This Thesis

The worth of this project lies, for the most part, in its exploration into using a particular type of computer simulation to examine [starting at the molecular level] the glass transition of a pure polymer and the glass transition of a polymer subject to CO_2. As a result this thesis will include some of the problems encountered along the way and subsequent solutions that would otherwise be omitted in a discussion of the results. The reason for doing this is two-fold; presenting encountered problems will provide insight into the complexity of using computer simulation and

also provide the context to discuss current work and recommendations for further work. As this research is still in progress, the later will be a large portion of the concluding sections.

This thesis is organized as follows. To begin, a brief overview of the computer simulation is given. This section includes no technical details of the code used but does attempt to illustrate fundamental simulation concepts, as well as provide the general algorithm employed to simulate the molecular motion/rearrangement that allows for *equilibrium* properties of the system to be probed [note: in many cases the system explored will exists in an away-from-equilibrium state (i.e. glass) and therefore this is really only a pseudo equilibrium state]. Next, the specifics of the simulated polymer are considered and the results of a cooling simulation are presented. From this cooling simulation the Glass Transition Temperature of the computer simulated polymer is found. The next logical step is the introduction of CO_2. An account of the problems encountered when CO_2 was introduced, the re-evaluation of the pure polymer T_g at higher pressures, and the results of CO_2-polymer cooling simulations are given in sections three through five. As it is difficult to confidently extract information on the glass transition of the polymer subject to CO_2 from the original properties recorded, a pseudo diffusion coefficient is examined. This is the topic of the sixth section. Finally, in the concluding sections recently obtained and, for the most part, unanalyzed results are given and future steps are suggested.

1. Simulation

The code used is designed to perform various molecular level simulations of spherical particles. In this simulation, particles [molecules] occupy a position in the simulation *box* and interact as dictated by a spherical potential [the simulation box is the volume occupied by the simulated molecules]. For this research project the Lennard-Jones potential was used to describe intermolecular interactions. Figure 4 gives a rough picture of a simulation containing five particles. Figure 5 shows a Lennard-Jones potential curve fitted to empirical results.

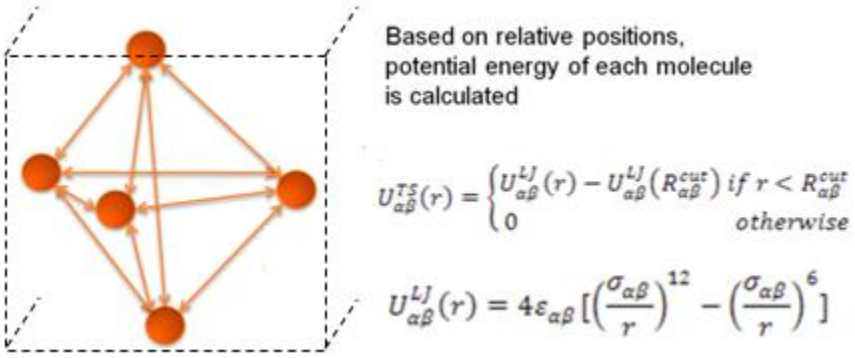

Figure 4: Cartoon of simulation containing five particles

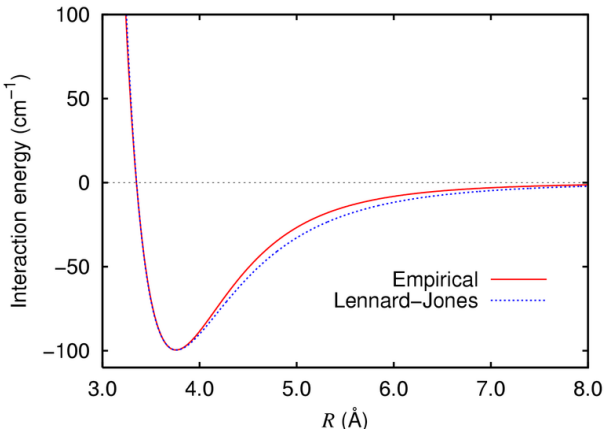

Figure 5: Interaction energy of argon dimer. Empirical results taken from R. A. Aziz, J. Chem. Phys., vol. 99, 4518 (1993), Lennard-Jones fitted to the empirical results (Poszwa, 2005) (Aziz, 1993).

The general form of the Lennard-Jones potential is the following:

Equation 1

$$U_{\alpha\beta}^{LJ}(r) = 4\varepsilon_{\alpha\beta}[\left(\frac{\sigma_{\alpha\beta}}{r}\right)^{12} - \left(\frac{\sigma_{\alpha\beta}}{r}\right)^{6}]$$

Although the Lennard-Jones potential is in part derived from theory, the full form has been obtained by fitting an equation to empirical interaction data. In this equation, epsilon (ε) is the parameter in which the strength of interactions is specified and thus corresponds to the depth of the potential well [E.g. for non-polar molecules such as halogens, which exist naturally as diatomic molecules, the greater London dispersion interaction between the larger I_2 molecules compared to the smaller Cl_2 molecules will manifest in a larger epsilon]. Sigma (σ) is the distance at which the molecules in question neither attract nor repel each other [i.e. the position of the bottom of the potential well], and is consequently taken to be the size of the particle. The portion raised to the 12th power ($(\sigma/r)^{12}$) describes the short range region in which the molecules experience repulsion due to electron orbital overlap [Pauli repulsion], leaving $(\sigma/r)^6$, which describes the long range region where molecules are attracted to each other via Van Der Walls forces. Thus, in simulation, a molecule is defined by assigning the particle size, strength of interaction and distance at which the interactions become negligible (Rcut).

Furthermore, polymers are modeled using a bead-spring model in which particles representing polymer segments are connected by a spring potential (Equation 2). Figure 6 provides a visual reference.

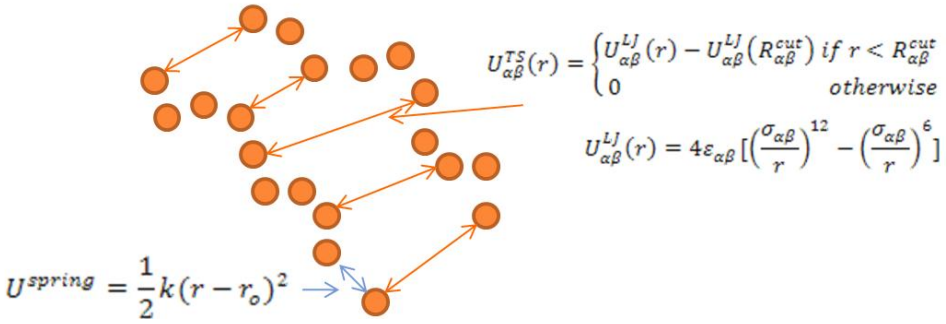

Figure 6: Simulation of polymers

Equation 2

$$U^{spring} = \frac{1}{2}k(r - r_o)^2$$

The strength of the covalent bond holding the segments together is represented by the spring constant, k, while the bond length is expressed as the natural length, r_o. Once the particle and polymer characteristics have been defined, a set number of polymers or particles are assigned positions in the simulation box. The rearrangement that would result [in *real* systems] from intermolecular interactions and molecular translational energy can then be simulated using a Monte Carlo (MC) technique or Molecular Dynamics (MD).

Simulating Molecular Motion/Rearrangement

monte carlo simulation.

In a MC simulation the following steps are taken:

Step 1: Positions for each particle in the simulation box are randomly generated. Using this configuration the potential energy is calculated.

Step 2: One particle or a portion of the polymer is chosen at random and given a new position in the box. For small molecules – as opposed to polymer segments – which are not connected to each other via a spring potential, this movement is more or less random [there is a slight restriction on the size of the movement most likely attempted]. To rearrange polymer segments, whose movements are somewhat

restricted, an end portion of the polymer is deleted and randomly re-grown on either side of the remaining chain.

Step 3: After one of these moves is made, the potential energy is recalculated for the new configuration. If the potential energy decreased or remained the same the random move is accepted. Otherwise the move is accepted with a probability given by $P_{accept\ move} = e^{-\frac{\Delta U}{k_b T}}$. These steps are depicted in the following two figures (Figure 7 and Figure 8).

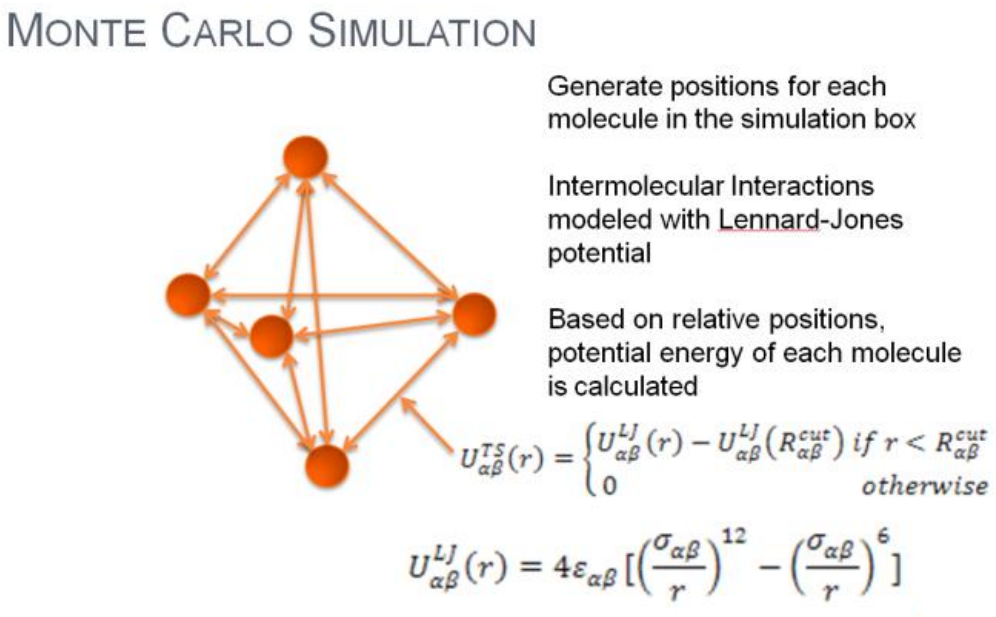

Figure 7: MC simulation step 1

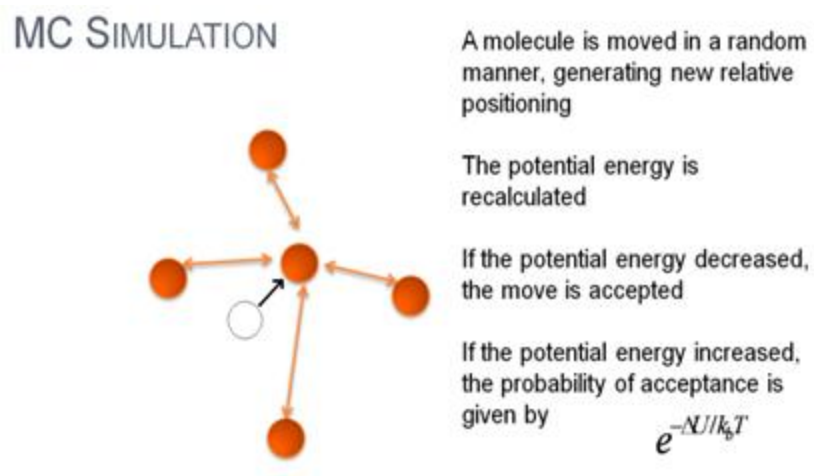

Figure 8: MC simulation steps 2 and 3

In this way the Monte Carlo simulation *equilibrates* the system. The thermophysial properties, at equilibrium are then computed by averaging.

molecular dynamics simulation.

In a MD simulation the particles are again given a position in the simulation box, however, a momentum distribution must be established based on temperature and, instead of rearranging the particles based on random movements and energy recalculation, molecular motion is described by Newton's equation of motion. No MD simulations were performed in this project.

Temperature, Pressure, Volume and Boundary Conditions in Simulation

temperature.

On a molecular level, temperature may be interpreted as a measure of the kinetic energy of molecules. In a MC simulation the effects of temperature are captured by accepting random moves that increase the potential energy with a probability of $P_{accept\ move} = e^{-\frac{\Delta U}{k_b T}}$. Thus, as expected, at high temperatures where the average molecular kinetic energy is high, intermolecular interactions only have a small effect on the rearrangement of molecules, and moves are likely to be accepted regardless of the change in potential energy.

pressure and volume.

In this project, simulations are run at a fixed temperature, pressure and number of total molecules. As a result the volume must be allowed to fluctuate and reach the corresponding equilibrium volume. Consider the easily understood example of an ideal gas in which the equation of state, PV =nRT holds. In this case, setting the pressure, temperature and number of molecules clearly sets the equilibrium volume [V = nRT/P]. Although, for many systems the equation of state may be very [prohibitively] complicated, setting pressure, temperature and the number of molecules still dictates the equilibrium volume of that system. That is to say, for any system the volume must be such that, at the given temperature, the pressure exerted on the surroundings equals the pressure exerted by the surroundings on the system [in simulation this pressure must be equal to the set pressure]. This is illustrated in Figure 9: the following cartoon.

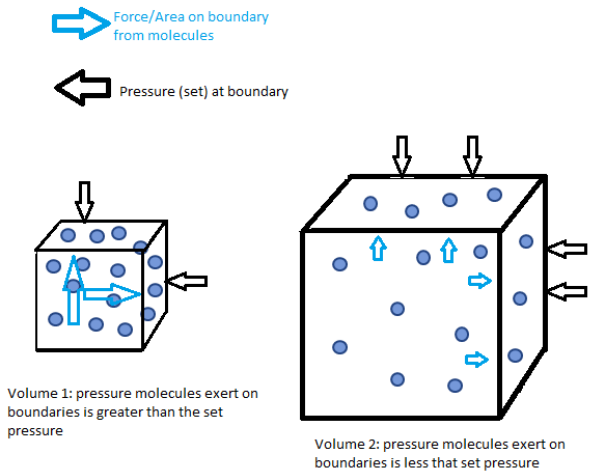

Figure 9: Qualitative depiction of the equilibrium that must exist between the number of molecules, temperature [although this is difficult to illustrate here], volume and pressure. At the equilibrated volume the pressures must be equal.

Although, it was mentioned that volume was allowed to fluctuate in a Monte Carlo simulation, to this point only molecular rearrangement has been discussed. For a MC simulation to be accurate [and useful], the above equilibrium constraint must be captured. To do this, volume is changed in a manner similar to molecular rearrangement: For a given configuration, the volume [size of the simulation box] is

changed in a random manner. If the volume is decreased, the system is compressed; if the volume is increased, the system is expanded. Consider the case where volume decreases – illustrated in Figure 10 below.

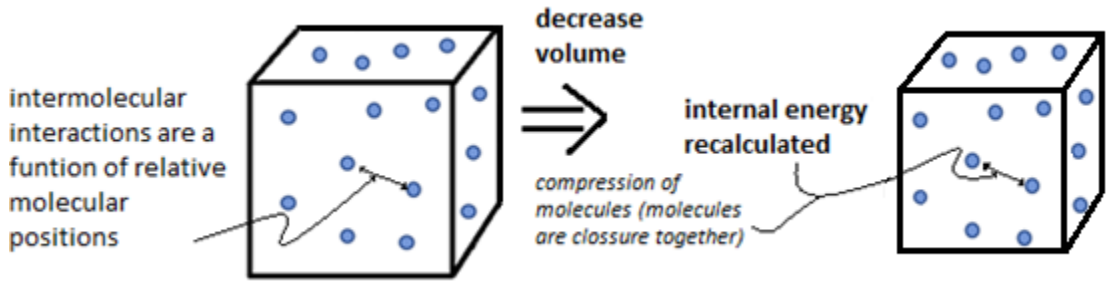

Figure 10: Illustration of volume change

This move is accepted if an enthalpy-like quantity is reduced [rather than just potential energy from the intermolecular interactions as was the case when molecules were rearranged]. Specifically when

$$\Delta H_{MC}|_P = P\Delta V_{MC} + \Delta U_{MC} \leq 0$$

Where ΔV_{MC} is the attempted change in volume and ΔU_{MC} is the associated change in potential energy as dictated by the intermolecular interactions.

If the pseudo enthalpy is not reduced, then the volume change is accepted with a probability equal to

$$P = e^{\frac{-P\Delta V}{k_b T}} e^{\frac{-\Delta U}{k_b T}} = e^{\frac{-\Delta H}{k_b T}}$$

Again, in this way, the effects of temperature are incorporated in the volume fluctuations.

boundary conditions in simulation.

Although only a relatively small number of molecules are placed in the simulation box, these molecules are treated as molecules occupying a very small

volume element in a much larger homogeneous bulk phase by applying a periodic boundary condition. That is, intermolecular interactions are calculated as if [shown in Figure 11] the simulation box is surrounded by boxes containing molecules in the exact same orientation.

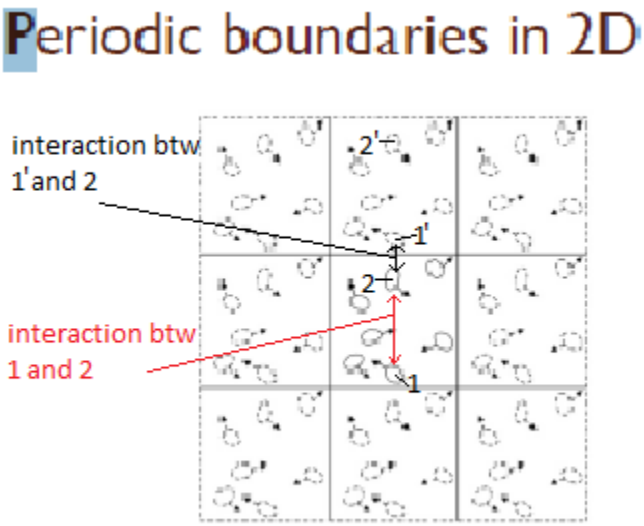

Figure 11: Classic Depiction of a periodic boundary condition in 2D

Note that this restricts the simulation box size with respect to the cut off distance [the distance at which intermolecular interactions are taken to be zero] – the length of the box side must be larger than R_{cut}.

Reduced Critical Temperature and Pressure and Molecule Parameters

In order to parameterize the molecules of interest the reduced critical temperature and pressure must be found. The following briefly describes how this is done and how these quantities relate to the parameters that are used to characterize molecules in simulation.

Equations of states for fluids are primarily dictated by intermolecular interactions. This being the case, the temperature at which the gaseous state and liquid state properties are no longer distinguishable [i.e. the Critical Temperature] must also be primarily a function of the intermolecular interactions. In simulation

the Critical Temperature of a fluid must be a function of ε, the parameter that specifies the strength of intermolecular interactions.

$$T_c = f(\varepsilon)$$

Furthermore an "interesting fact that has emerged from the study of molecular behavior [i.e. statistical mechanics] is that as far as molecular interactions are concerned, molecules can be grouped into classes, such as spherical molecules, non-spherical molecules, molecules with permanent dipole moments and so forth, and that within any one class, molecular interactions are similar" (Sandler, 2006). It's therefore reasonable to assume that, within a class of molecules, the critical temperature is approximately proportional to the strength of interaction. In simulation the functional form of the intermolecular interaction potential is the same for each molecule [spherical molecules with intermolecular interaction described by a LJ potential] and the ratio T_c and ε is a constant.

$$T_c \propto \varepsilon$$
$$\frac{T_c}{\varepsilon} = C$$

This means the reduced Critical Temperature, T_c^* is a constant, for computer simulated molecules.

Equation 3

$$T_c^* = \frac{k_B T_c}{\varepsilon} = C1$$

For interactions used in this computer simulation, the reduced Critical Temperature is found by plotting the density of the liquid and gaseous phases vs. reduced temperature. At the reduced Critical Temperature these two densities are equal.

The reduced Critical Pressure may be found in a similar manner. Furthermore, P_c is primarily a function of the intermolecular interactions and size of

the molecules and therefore, in simulation must be a function of ε and σ. To be more specific, the following is true in simulation.

Equation 4

$$P_c^* = \frac{P_c}{\varepsilon / \sigma^3} = C2$$

With these relations (Equation 3 and Equation 4) characteristic LJ parameters can be found for molecules or polymers of interest.

2. Simulating a Polymer

Polymer Parameters

As previously mentioned, polymers are composed of spherical segments connected by a harmonic spring potential.

Equation 2

$$U^{spring} = \frac{1}{2}k(r - r_o)^2$$

In which k, the spring constant, allows the user to specify the strength of the *bond* holding the polymer segments together and r_0, the natural length, allows the user to specify the center-to-center distance at which the connected segments impart no force on each other. These constants are made dimensionless as follows:

$$k^* = \frac{k * (\sigma_{polymer})^2}{\varepsilon_{polymer}}$$

$$r^* = \frac{r}{\sigma_{polymer}}$$

Where $\sigma_{polymer}$ is the characteristic size of a polymer segment and $\varepsilon_{polymer}$ is the parameter used in to indicate the strength of intermolecular interactions between non-connected polymer segments.

A dimensionless spring constant of 800 and a dimensionless natural length of 1 are used to define the covalent bond connecting the polymer segments. Furthermore, segments are tangentially attached with no constraints on bond angles and the polymer is restricted to a 10 segment chain [longer chains increase computation time]. Again, the interactions between non-connected polymer segments are defined by a truncated and shifted Lennard-Jones potential.

Equation 5

$$U_{\alpha\beta}^{TS}(r) = \begin{cases} U_{\alpha\beta}^{LJ}(r) - U_{\alpha\beta}^{LJ}\left(R_{\alpha\beta}^{cut}\right) \; if \; r < R_{\alpha\beta}^{cut} \\ 0 \qquad\qquad\qquad\qquad otherwise \end{cases}$$

Where the subscripts α and β denote the species, $R_{\alpha\beta}^{cut}$ is the cut-off distance, and $U_{\alpha\beta}^{LJ}(r)$ is the Lennard-Jones potential, which, as shown before, is defined by

Equation 1

$$U_{\alpha\beta}^{LJ}(r) = 4\varepsilon_{\alpha\beta}[\left(\frac{\sigma_{\alpha\beta}}{r}\right)^{12} - \left(\frac{\sigma_{\alpha\beta}}{r}\right)^{6}]$$

Quick note: From this point forward, the subscript β will be used to indicate a polymer segment the subscript α will be used to indicate a CO_2 molecule. That is $\varepsilon_{\beta\beta}$ characterizes the strength of polymer segment-segment intermolecular interactions, $\varepsilon_{\alpha\beta}$ describes CO_2-polymer interactions etc.

To parameterize the simulated polymer interactions such that the model represents a *real* long-chain molecule, the critical temperature and pressure of the alkane polymer (C_{28}) were used to find $\varepsilon_{\beta\beta}$ and $\sigma_{\beta\beta}$ [recall the relations given (Equation 3 and Equation 4)].

Equation 3

$$\varepsilon_{\beta\beta} = \frac{k_B T_C}{T_C^*}$$

Equation 4

$$\sigma_{\beta\beta} = \left(\frac{P_C^* \varepsilon}{P_C}\right)^{1/3}$$

T_C and P_C are the critical temperature and pressure of C_{28} respectively
T_C^* and P_C^* are the dimensionless [reduced] critical temperature and pressure found from simulation (see intro, reduced critical P and T).

$\varepsilon_{\beta\beta}$ = 5.455x10^{-21} J and $\sigma_{\beta\beta}$ = 3.797 Å (Talreja, 2010). The cut off distance is 2.5 x $\sigma_{\beta\beta}$ giving an R_{cut} of 9.4925 Å.

Obtaining the T_g of a Pure Polymer Via MC Simulation

Once a polymer has been parameterized, simulations can be run to elicit information about the glass transition of that Polymer. To do this, a series of isobaric-isothermal MC simulations are performed, starting at a high temperature and stepping down in 10 K intervals. Obtaining the equilibrium density or volume at each temperature allows for the determination of a transition state in which the polymer interactions, orientation and movements no longer describe a liquid state but instead suggest a more rigid or glassy state. The temperature at which this transition occurs is found by plotting the volume for each isobaric-isothermal MC equilibration vs. temperature. Upon plotting it should become clear under what temperatures the system exists in a glass like state – a state in which the change in volume per change in temperature is relatively low – and under what temperatures the system exists in a liquid like state – a state in which the change in volume per change in temperature is relatively high [compared to the glassy state]. The temperature, then, that corresponds to a substantial change in dV/dT is the Glass Transition Temperature, Tg.

The details of the first MC polymer cooling simulation are as follows. 100 polymer chains [1000 segments] were assigned a position in the simulation box and a MC simulation was performed, setting the temperature to 300 K and the pressure to 1 atm. After 20,000 MC *moves* the rearranged configuration was copied and used as the starting configuration for the next MC simulation, this time run at 290 K and, again, at atmospheric pressure [in a single *move* a random rearrangement is tried, on average, for *each* molecule or polymer segment in the simulation box]. This process was repeated, decreasing the temperature by 10 K for each subsequent simulation until 80 K was reached. Although, the configuration used for the next simulation was copied after 20,000 MC moves, to obtain a better statistical sampling of the polymer properties, each simulation was allowed to run for an additional 380,000 MC moves. As discussed early, the temperature at which the polymer transitions from glass to liquid may be found upon plotting the volume vs. temperature and is made apparent by a change in slope. However, as vitrification is distinctly different from a phase change in that the transition occurs gradually,

rather than at a given temperature, the bulk polymer properties become somewhat blurred around the Glass Transition Temperature – displaying properties that are not indicative of a glass or a liquid. In fact, upon first examination it appears that the transition from liquid to glass occurs somewhat smoothly (Figure 12).

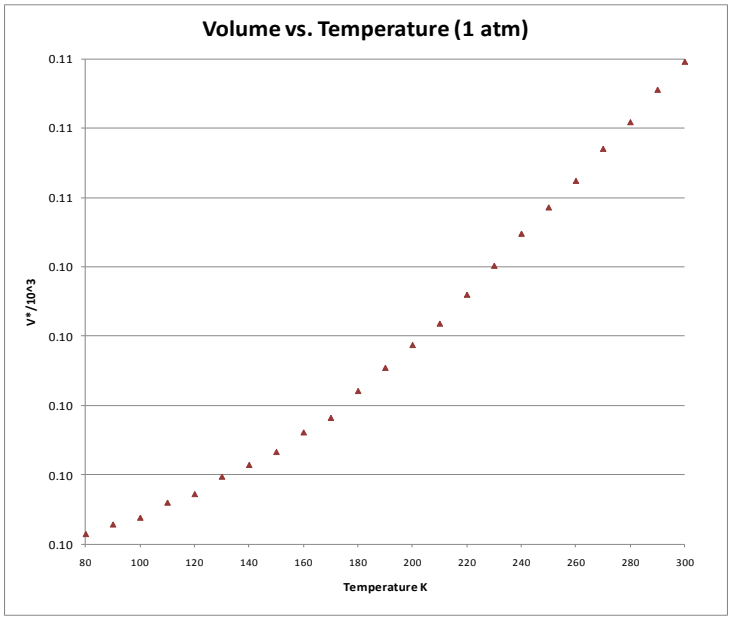

Figure 12: Volume of pure polymer vs. temperature at atmospheric pressure

In an attempt to determine the glass transition region, the *slope* at each point is plotted vs. temperature (Figure 13) [the *slope* at each point is taken to be the slope of a line fit to the point in question and the two neighboring points].

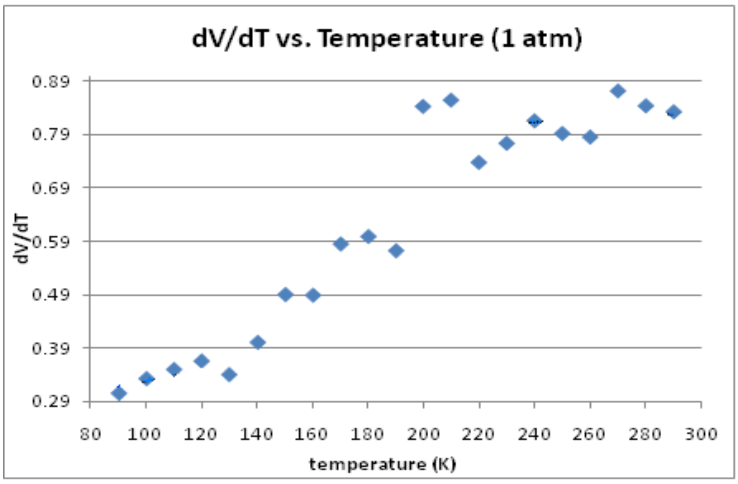

Figure 13: Dv/dT vs. temperature

Again, the region that shows a substantial change in slope corresponds to the glass transition region. However, there is still not such a sharp change so as to leave little room for debate as to whether or not the regions are evident from this plot. One interpretation of this graph is as follows.

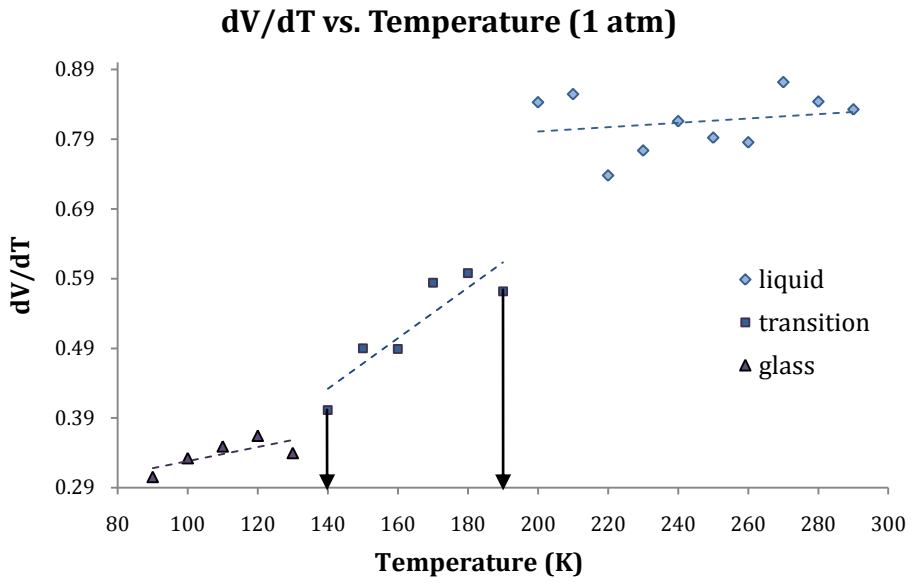

Figure 14: Plotting dV/dT vs. temperature suggests a glass transition region of ~ 140 K to 190 K.

In order to conduct a more rigorous analysis and to justify breaking this curve into three distinct regions [liquid, transition, and glass] a brief statistical analysis was performed.

statistical analysis of the pure polymer volume curve.

In the following analysis it is assumed that the volume observed at each temperature is taken from a population of possible values, which are normally distributed about the true mean. As explained by the central limit theorem, this assumption is valid if the deviation from the true mean is the additive result of a number of unknown or uncontrollable variables giving the appearance of random error. Central Limit Theorem: "if y_1, y_2, … y_n is a sequence of n independent random

variables from a population [which might or might not be normal] with a mean μ and a variance σ^2, then the sum of the y-values will be approximately normally distributed as"

$$\frac{\sum_i^n y_i - n\mu}{\sqrt{n\sigma^2}} \sim N(0,1)$$

Note: the notation X ~ F means "X belongs to the F distribution"

In simulation this assumption should be valid, as the deviation from the true mean is the cumulative [additive] result of a number of variables including random effects from the initial configuration and MC movements.

Probability density functions (pdf) of statistics derived from samples of normally distributed data are known. This allows for conjectures to be made about the true population parameters and provides a pathway to examine the effects of different factors on the dependent measured variable [e.g. effects of temperature *and state* on the volume].

The F-statistic and corresponding distribution (Equation 6) can be used to compare deviations of samples.

Equation 6

$$\frac{S_2^2/\sigma_2^2}{\frac{(n2-1)}{S_1^2/\sigma_1^2}} \sim F_{n2-1,n1-1}$$
$$\frac{}{(n1-1)}$$

Where S_i is the standard deviation of sample$_i$, σ_i is the true population deviation and n_i is the number of collected data points in sample$_i$.

Thus, given two sample deviations, the hypothesis $\sigma_1 = \sigma_2$ can be tested [this type of hypothesis is often referred to as the null hypothesis].

If $\sigma_1 = \sigma_2$, then Equation 7.1 is true

Equation 7.1 [eqn. 7 when $\sigma_1 = \sigma_2$]

$$\frac{\frac{S_2^2}{(n2-1)}}{\frac{S_1^2}{(n1-1)}} \sim F_{n2-1,n1-1}$$

Therefore we can determine the probability that the two samples were collected from populations having the same deviation.

This result can be extended to compare effects of known factors [in this case the effects of temperature and state] with the effects of *random* error using Analysis of Variance (ANOVA). For the sake of simplicity consider the following continuous factor effects model

$$V = \beta_0 + \beta_1 T + \varepsilon \; ; \varepsilon \sim N(0, \sigma^2)$$

This model predicts that temperature has an effect on volume – V vs. T is linear with deviations from this line resulting from random error. If, however, this model is not significantly better than the null model, then any deviation from a constant value across varying temperatures should be solely due to random error. The null model is mathematically expressed by the following equation

$$V = \beta_0 + \varepsilon \; ; \varepsilon \sim N(0, \sigma^2) - null\ model$$

ANOVA gives the probability that the observed variance across varying factor levels [e.g. across a range of temperatures] is due to random error or unaccounted for factors rather than the modeled effects. This is accomplished via the ratio of model deviation to random error obtained in the following way

$$SS_{Model} = \sum_{i=1}^{N} (\hat{V}_i - \bar{V}_{\circ\circ})^2$$

$$SS_E = \sum_{i=1}^{N} (\hat{V}_i - V_i)^2$$

$\hat{V}_i$ is the predicted (from the continuous factor effects model) dependent variable, volume; $\bar{V}_{\circ\circ}$ is the average over all temperatures; V_i is the value of the i^{th} observed volume

Dividing the by the degrees of freedom gives the following defined quantities

$$\text{Define: } MS_{Model} \equiv \frac{SS_{Model}}{k} \; and \; MS_E \equiv \frac{SS_E}{n-k-1}$$

Here MS_E is a pooled estimate of the common variance – that is the variance from the predicted values given by the continuous factor effects model – and provides an estimate of σ^2. If the factor explored [temperature] has no effect on the dependent variable [volume] then MS_{model} also provides an estimate of σ^2. If this is the case the ratio of MS_{Model} to MS_E follows an F distribution

Equation 7.2 [plugging in SS and MS to eqn. 7]

$$\frac{\frac{SS_{Model}/\sigma^2}{(k)}}{\frac{SS_E/\sigma^2}{(n-k-1)}} = \frac{MS_{Model}}{MS_E} \sim F_{k,n-k-1}$$

This gives the probability that the sample data was collected from a population in which the only deviation from the true mean is due to random error or unaccounted-for factors. A low probability here, suggests that temperature does in fact have an effect on the volume.

As seen, a model is required prior to statistical analysis. The model used for the volume curve shown in Figure 12 must be physically reasonable and therefore the form of the mathematical model is partially constrained. Specifically, a higher than 2nd order temperature effect seems unlikely and only three distinct regions

associated with glass transition are expected. With this in mind, the following model is proposed

$$V = \mu + \tau_i + \beta_0 T + (\tau\beta_0)_i T + \beta_1 T^2 + \varepsilon;\ \varepsilon \sim N(0, \sigma^2)$$

$_i$ *denotes the state*

This model predicts that volume changes with temperature [not necessarily linearly] and that state [liquid, transition or glass] has an effect on dV/dT, as originally hypothesized.

For this research project a significance level (α) of .05 will be used. Note that in order to test this model, state must be designated for each temperature. To do this, the curve was arbitrarily broken into liquid, transition and glass regions; the separation that gave the best fit [or a second order polynomial] within each region was used. To perform the described statistical analysis, the computer software, JMP was used. The results are given on the following page (Figure 15).

Response Volume

Regression Plot

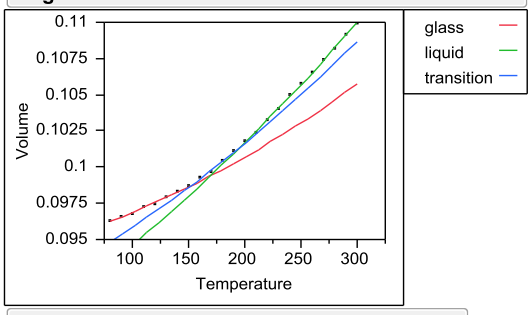

Analysis of Variance

Source	DF	Sum of Squares	Mean Square	F Ratio
Model	6	0.00041976	0.000070	12357.06
Error	16	9.05855e-8	5.662e-9	Prob > F
C. Total	22	0.00041985		<.0001*

Parameter Estimates

Term	Estimate	Std Error	t Ratio	Prob>|t|
Intercept	0.1007313	8.523e-5	1181.9	<.0001*
state[glass]	-0.000475	0.000111	-4.28	0.0006*
state[liquid]	0.0001855	0.000055	3.37	0.0039*
Temperature(80,300)	0.0066642	0.000127	52.49	<.0001*
Temperature*state[glass]	-0.001909	0.000383	-4.99	0.0001*
Temperature*state[liquid]	0.0016515	0.000409	4.04	0.0010*
Temperature*Temperature	0.000725	0.000294	2.46	0.0255*

Effect Tests

Source	Nparm	DF	Sum of Squares	F Ratio	Prob > F
state	2	2	0.00000011	9.5607	0.0019*
Temperature(80,300)	1	1	0.00001560	2755.457	<.0001*
Temperature*state	2	2	0.00000015	12.8143	0.0005*
Temperature*Temperature	1	1	3.43208e-8	6.0620	0.0255*

Effect Details

state

Least Squares Means Table

Level	Least Sq Mean	Std Error	Mean
glass	0.10025624	0.00018727	0.097205
liquid	0.10091674	0.00007982	0.105728
transition	0.10102081	0.00005849	0.099798

Temperature(80,300)

Temperature*state

Temperature*Temperature

Figure 15: Statistical analysis of the volume vs. temperature data obtained for the pure polymer at atmospheric pressure

In this summary, the Analysis of Variance tests the null hypothesis that no factors [temperature or state] *as modeled* effect the volume. Under the Analysis of Variance tab the p-value [under Prob > F in the summary] is the probability that the found statistic value could be observed if the null hypothesis is true. This value is less than .05 (α), rejecting the null hypothesis. Thus we can conclude that either state or temperature [or both] has a significant effect on volume. The Effects Tests tab shows the results concerning the statistical significance of each effect – each modeled effect is significant. Finally, the Parameter Estimates tab gives the results concerning the statistical significance of each parameter – all parameters are significantly different from zero.

To summarize, this test indicates that temperature has a significant effect on the observed volume, *and* that the state of the polymer has a significant effect on the rate of change of volume with changing temperature. Although this analysis, to an extent, justifies the use of the volume vs. temperature curve in determining a glass transition temperature *range*, it does not justify defining a single temperature as *the* Glass Transition Temperature, T_g.

For the sake of defining a single temperature to indicate the glass transition, the temperature at which the linear least square lines fit to the glass and liquid regions intersect will be denoted as the T_g. This seems to be common practice and has the benefit of minimizing the error in specifying the regions [changing the state designation around the transition temperatures only slightly shifts the intersection temperature]. The Glass Transition Temperature [defined in this way] for the computer-simulated polymer at atmospheric pressure is ~ 172 K, as shown in the following figure, Figure 16.

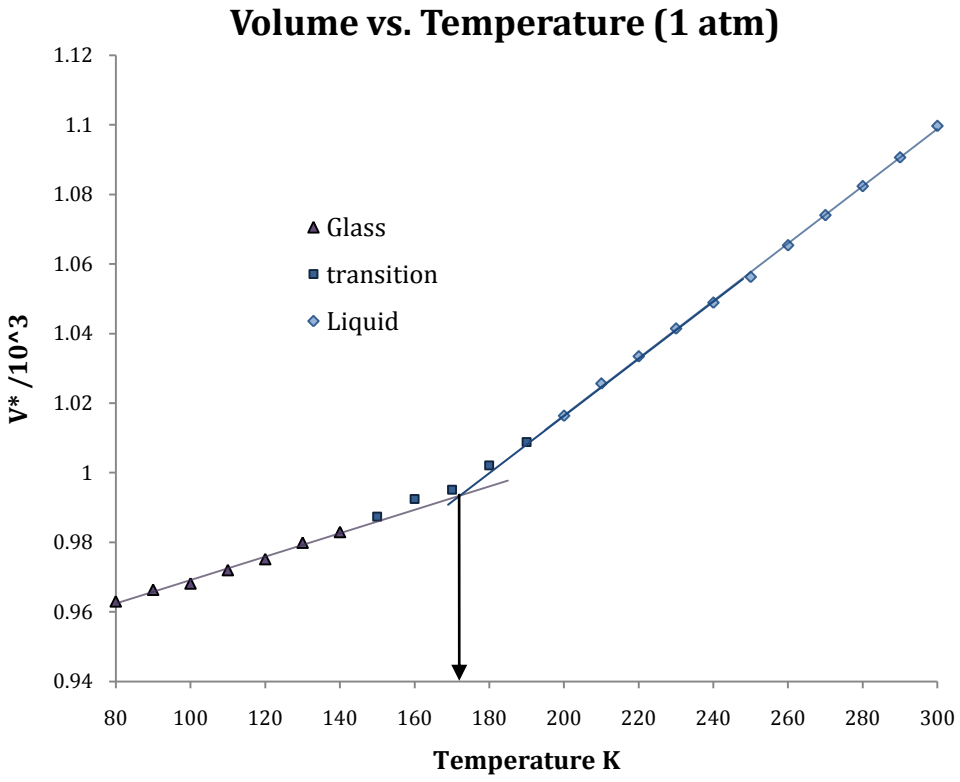

Figure 16: Plotting the volume vs. temperature obtained via a MC cooling simulation indicates a Tg of ~ 172K at atmospheric pressure.

3. Introducing CO_2

Two-box Simulation

To this point molecules have filled a single simulation box, which only allows for the study of a homogeneous single phase pure substance or mixture of a set composition and cannot be used to study, for example, the interaction of CO_2 gas with plastic. To subject the system of polymers to small molecules existing in a fluid state [e.g. gaseous CO_2], a two-box simulation must be implemented. As the name suggests, in this type of simulation two simulation boxes are used – one containing CO_2 and the other containing the polymer. During MC equilibration the CO_2 molecules are allowed to move between the boxes, however, the polymer is constrained to a single box. This simulates a plastic substance subject to CO_2, which dissolves in the plastic or escapes from the plastic until equilibrium is established. Figure 17 gives a snap shot of the two-box simulation. The polymer segments are shown in red and the CO_2 molecules are given in blue.

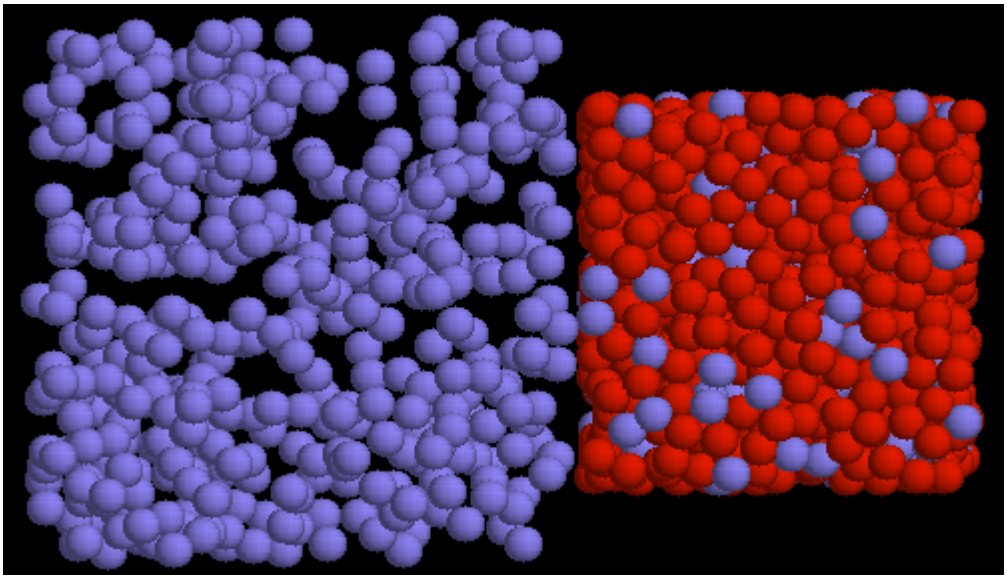

Figure 17: Two-box simulation (polymer segments - red; CO_2 molecules - blue)

"Parameterizing" CO_2

To explore the effects of CO_2 on the Glass Transition Temperature of a polymer, computer simulated molecules must be parameterized to represent CO_2.

This is done – as with the polymer – using the critical temperature and pressure of CO_2 (7.375 MPa and 304.13K respectively), and the relations given in Equation 3 and Equation 4. Yielding an $\varepsilon_{\alpha\alpha}$ = 3.9153 x 10^{-21} J and an $\sigma_{\alpha\alpha}$= 3.6738 Å. The cut-off distance, R_{cut}, is taken to be 2.5 x $\sigma_{\alpha\alpha}$ or 9.1845 Å.

cross interactions.

So far only pure substance intermolecular interactions have been parameterized, however, with the introduction of CO_2 cross-interactions like those illustrated in Figure 18 must be parameterized.

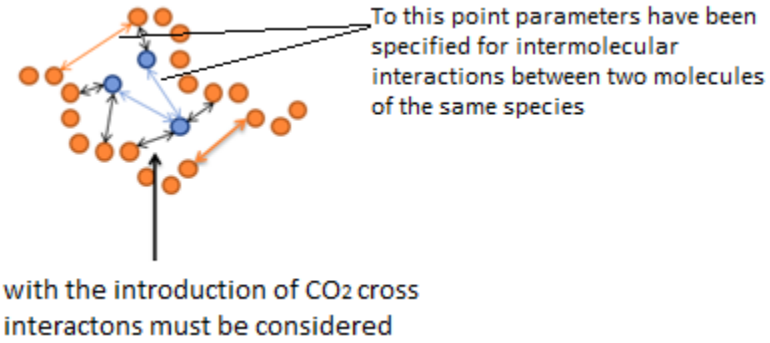

Figure 18: Depiction of cross interactions in mixtures

Recall that characteristic parameters for intermolecular interactions in a pure substance where obtained via the critical temperature and pressure. This information, however, is less available for mixtures. Fortunately, cross interaction parameters may be roughly found from the pure substance interaction parameters using the so-called Lorentz-Berthelot (LB) mixing rules. These are as follows:

$$\sigma_{\alpha\beta} = k_\sigma \frac{\sigma_{\alpha\alpha} + \sigma_{\beta\beta}}{2}$$

$$\varepsilon_{\alpha\beta} = k_\varepsilon \sqrt{\varepsilon_{\alpha\alpha}\varepsilon_{\beta\beta}}$$

Figure 19: Lorentz-Berthelot mixing rules

k_σ and k_ε are adjustment parameters

For simplicity, k_σ is taken to be 1. Thus sigma, the parameter giving the particle diameter is simply the average of two interacting particles. k_ε is found by minimizing the following objective function.

$$f_{obj} = \sum_{i=1}^{m} (x_{CO_2}^{model}(i) - x_{CO_2}^{exp}(i))^2$$

In this function $x_{CO_2}^{model}$ is the mole fraction of CO_2 in the polymer-containing simulation box, whereas, $x_{CO_2}^{exp}$ is taken from experimental CO_2 solubility data for octacosane (Sato, Tagashira, Maruyama, Takishima, & Masuoka, 1998).

To find the k_ε value that minimizes f_{obj}, $x_{CO_2}^{model}$ data is obtained from simulations using k_ε values from 1 to zero, in increments of 0.0025. These simulations are performed at two temperatures (373.2K and 423.2 K) and a single pressure [thus m = 2]. This is illustrated in Figure 20

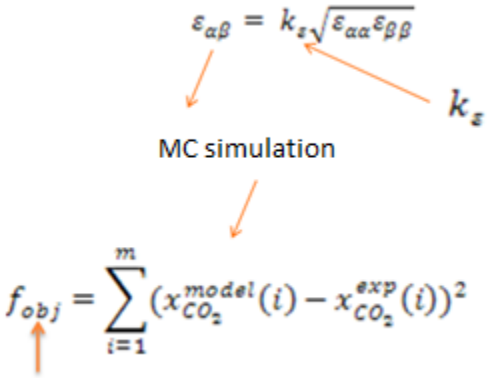

Figure 20: Finding the cross interaction epsilon adjustment parameter

f_{obj} is minimized at k_ε = .9525. Resulting in the parameters: $\sigma_{\alpha\beta}$= 3.735 Å and $\varepsilon_{\alpha\beta}$= 4.402 x 10^{-21} J (Talreja, 2010).

Once cross interaction parameters where established, simulations results where compared with experimental data by Dr. Manish Talreja, who found the

simulation to give fairly accurate solubility data over the range of pressures studied. Figure 21 compares experimental solubility data with simulation solubility data.

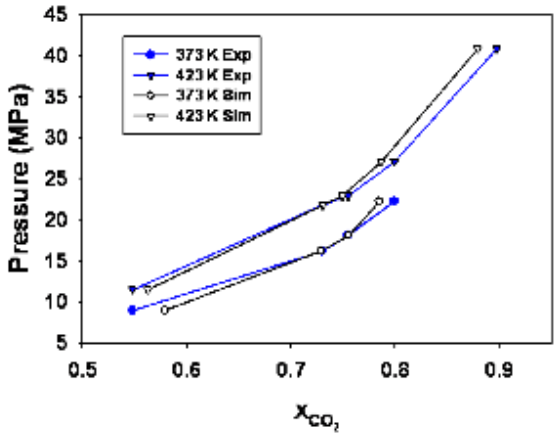

Figure 21: Solubility comparison between experimental data and results from a two-box simulation. (Talreja, 2010)

Initial Two-box Cooling Simulation

Originally, a cooling simulation – similar to the one taken to explore the pure polymer glass transition – was executed for the two-box simulation. The details are as follows. 600 CO_2 molecules were given an initial, random configuration in one box, while 100 polymer chains were given an initial, random configuration in the other box. The polymer and CO_2 molecules were then allowed to equilibrate using a MC simulation under isobaric-isothermal conditions at 300K and atmospheric pressure. After 20,000 MC moves, the new configuration is copied and taken as the starting configuration for the next simulation, which was run at 10 K lower. This process was repeated until 100 K was reached. Simulations at each temperature were run for an additional 2,000,000 MC moves to achieve a better estimate of equilibrium properties. However, very little CO_2 dissolved in the polymer at atmospheric pressure. Furthermore, when the pressure was increased to 5 MPa, the analysis was complicated by phase changes in the CO_2-box [It should be noted that at pressure of 5 MPa *real* CO_2 condenses and freezes at temperatures higher than the T_g observed for the simulated pure polymer]. While this complicates the initial experimental design, it also, partially validates the CO_2 model as the properties of

real CO_2 are reflected in simulation. This also suggests that CO_2 may only be used to assists in the described melding process if the T_g of the plastic nanostructures is above the critical temperature of CO_2.

Changing the CO_2 Parameters

In order to simulate plastic subject to supercritical CO_2 the simulation parameters must be changed. To do so without making past pure polymer results irrelevant, the CO_2 parameters are changed. However, this must be done in such a way that the simulated molecules are still representative of CO_2 but do not undergo phase transitions at or near the polymer T_g.

As Polystyrene (PS) is a polymer of particular interest for this research, we compared the T_g of polystyrene to the Critical Temperature of CO_2. The T_g of PS at atmospheric pressure is approximately 373.13 K, while CO_2 becomes supercritical at 304.13 K. This indicates that CO_2 is in fact supercritical at temperatures that melding PS nanostructures becomes possible. To simulate the behavior of *real* CO_2 at temperatures in the vicinity of the T_g of Polystyrene, the parameters were scaled in the following way

$$\frac{T_g(CS10mer)}{T_c(CS\ CO_2)} = \frac{T_g(PS)}{T_c(CO_2)} = 1.2268$$

Yielding $T_c(CS\ CO_2)$ = 138.56 K. The parameters may then be changed accordingly, following the relations used previously.

Equation 3

$$T_c^* = \frac{k_B T_c^{old}}{\varepsilon_{\alpha\alpha}^{old}} = \frac{k_B T_c^{new}}{\varepsilon_{\alpha\alpha}^{new}}$$

Giving a new computer simulated CO_2 interaction parameter, $\varepsilon_{\alpha\alpha}^{new}$= 1.784 x 10^{-21} J. And

Equation 4

$$P_c^* = \frac{P_c}{\varepsilon_{\alpha\alpha}^{old} / (\sigma_{\alpha\alpha}^{old})^3} = \frac{P_c}{\varepsilon_{\alpha\alpha}^{new} / (\sigma_{\alpha\alpha}^{new})^3}$$

Giving a new CS CO_2 size parameter, $\sigma_{\alpha\alpha}^{new}$ = 2.827 Å. This, of course, also changes the cross interaction parameters. For convenience, the same k_ε value was used [although less justified in this case] and k_σ was again taken to be 1. This gives the cross parameters, $\varepsilon_{\alpha\beta}^{new}$= 2.9714 x 10^{-21} J and $\sigma_{\alpha\beta}^{new}$ = 3.312 Å.

It should be noted that, not only does this scale the CO_2 parameters; this also loosely defines our system as representative of Polystyrene when subject to CO_2 at near glass transition temperatures.

4. Pure Polymer Glass Transition Temperatures at 10 MPa and 15MPa

As increased pressures are required to achieve the desired CO_2 solubility, the pure polymer was reexamined at pressures of 10 MPa and 15 MPa. Implementing the same MC cooling simulation produces the data presented in Figure 22-Figure 25.

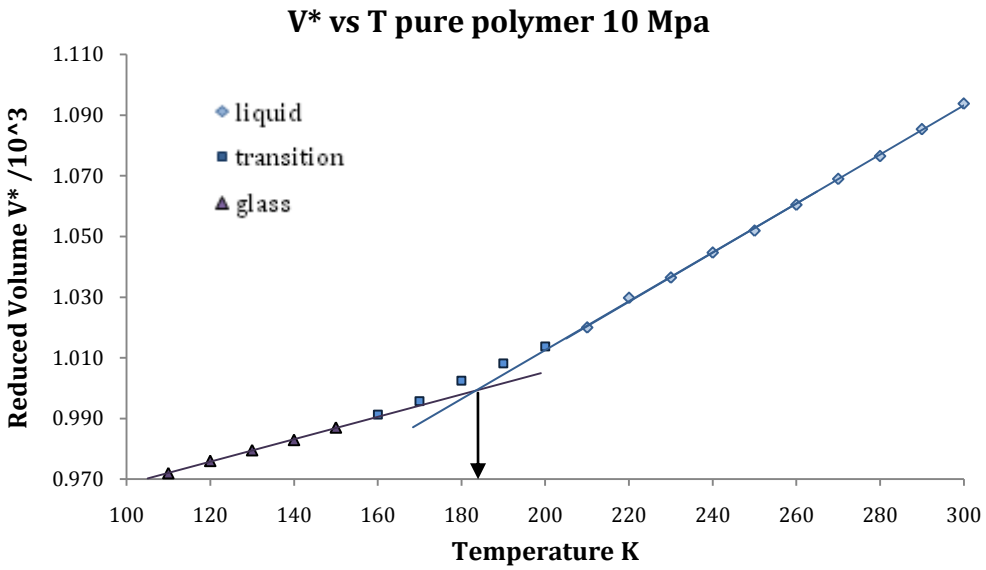

Figure 22: Volume vs. temperature for the pure CS polymer, at 10 MPa. Tg ~ 183 K

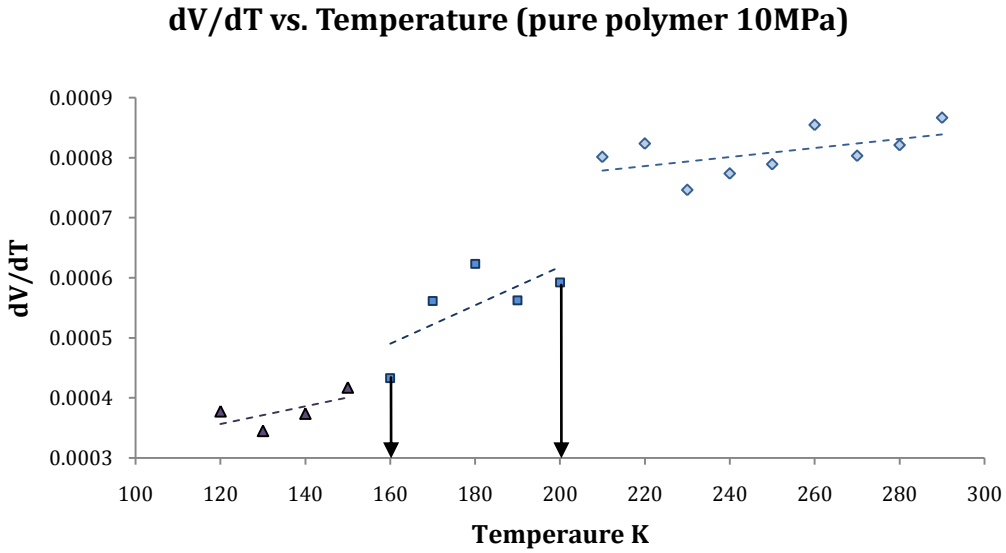

Figure 23: DV/dT vs. temperature for the pure CS polymer at 10 MPa. Glass Transition range ~ 160-200K.

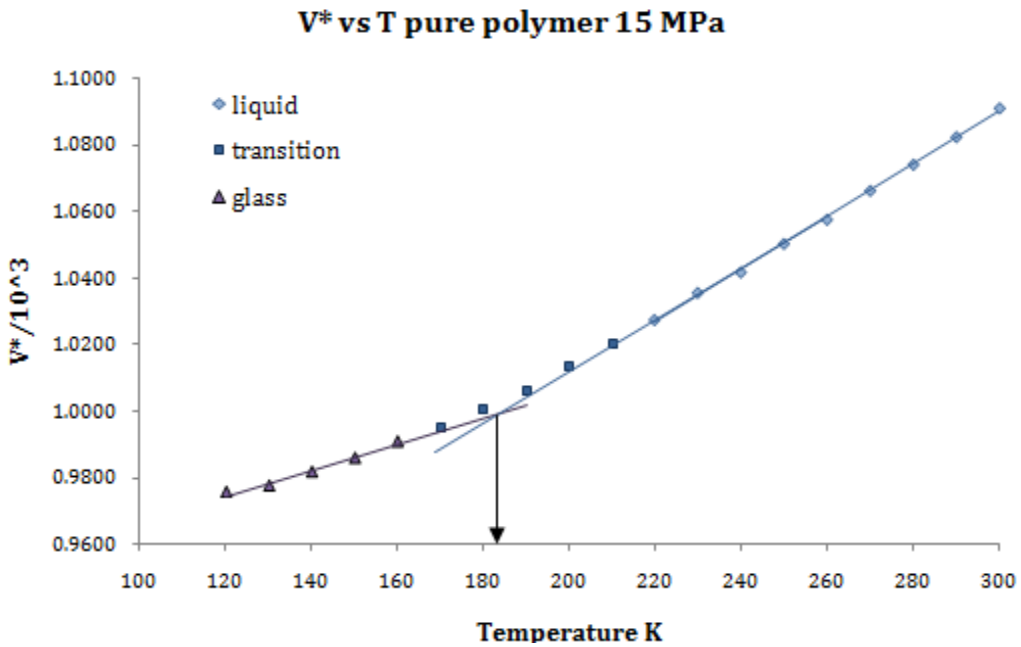

Figure 24: Volume vs. temperature for the pure CS polymer, at 15 MPa. Tg ~ 183

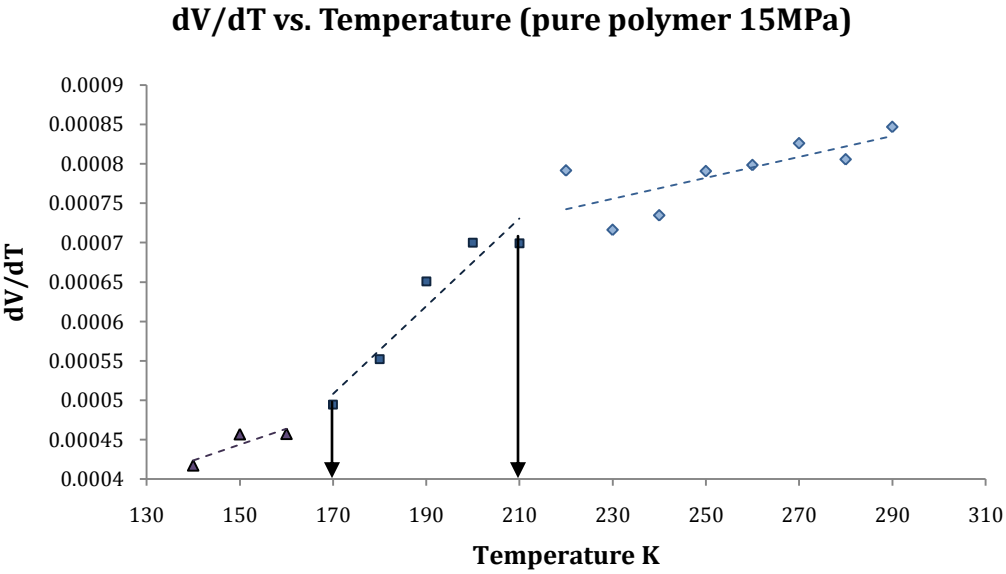

Figure 25: DV/dT vs. temperature for the pure CS polymer at 15 MPa. Glass Transition range ~ 170-210K.

A statistical analysis, similar to the previously described analysis [of the volume curve at atmospheric pressure] was performed on the data given in Figure 22 and Figure 24. The results of this analysis indicate that, at both pressures, state does have a statistically significant effect on the rate of change of volume with temperature. These results are provided in Appendix A.

The information on glass transition extracted from these curves is summarized in the following table, Table 1.

Table 1: Tg and Glass Transition Range for the pure CS polymer at different pressures

Pressure (MPa)	T_g (K)	Glass Transition Range (K)
.1	~172	140-190
10	~183	160-200
15	~183	170-210

As might be expected, the Glass Transition Temperature increases when the pressure is changed from atmospheric pressure to higher pressures. However, contrary to intuition, the T_g at 10 MPa appears to be about the same as the T_g at 15 MPa. There are a few reasons why this might be happening, namely, the relative difference between the two high pressures, 10 and 15 MPa is small [same order of magnitude] compared to the difference between .1 and 10 MPa [two orders of magnitude difference] and the method used to choose T_g may be washing out the more subtle effects of pressure. That is to say, the effect of this pressure difference on T_g is on the same scale as the natural variability associated with the computer simulation and this difference is then washed out when choosing a single temperature to be *the* Glass Transition Temperature. When examining the transition *range*, the transition appears to occur, as would be expected, at slightly higher temperatures for 15 MPa.

5. Finding the T_g of a Polymer with Dissolved CO_2

Extracting the Glass Transition Temperature of the CO_2-containing polymer isn't as straight forward as finding the T_g of the pure polymer. For the pure polymer, the Glass Transition Temperature [or, more accurately, glass transition region] is indicated by a change in the slope of volume plotted against temperature. Although temperature expansion effects are similar for the CO_2-polymer mixture – that is, the volume expansion of a CO_2-polymer mixture due to a temperature increase is greater in the liquid regime than in the solid regime – the volume vs. temperature plot is complicated by a non-constant amount of CO_2 in the polymer-containing box. Therefore, in an attempt to extract the glass transition temperature range, the CO_2 mole fraction, the overall number density [number of CO_2 molecules and polymer segments per volume] and the CO_2 number density in the CO_2-polymer box are also plotted against temperature. To confidently attribute trend changes in these plots to the polymer glass transition it is also important, as will be shown later, to plot the density of the pure CO_2 vs. temperature.

Two-box Simulation with New CO_2 Parameters

Using the adjusted CO_2 and cross-interaction parameters, additional MC two-box simulations were run. These simulations followed the same cooling procedure. From these simulations the mole fraction, number densities, and volume of the CO_2-polymer box are obtained at each temperature. These results are displayed in the graphs that follow. Figure 26-Figure 29 correspond to the cooling simulation run at 15 MPa, while Figure 30-Figure 33 correspond to the cooling simulation run at 10 MPa.

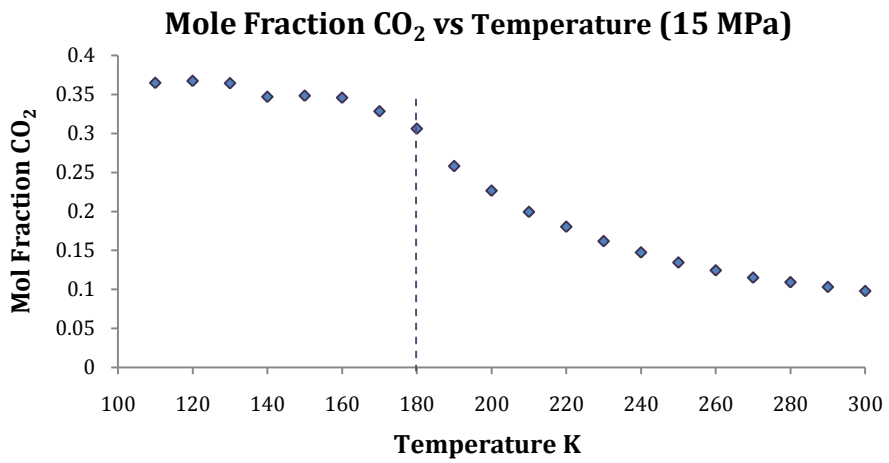

Figure 26: Gives the mole fraction of CO_2 in the CO_2-polymer box. From the 2-box cooling simulation, using the new CO_2 parameters run at 15 MPa

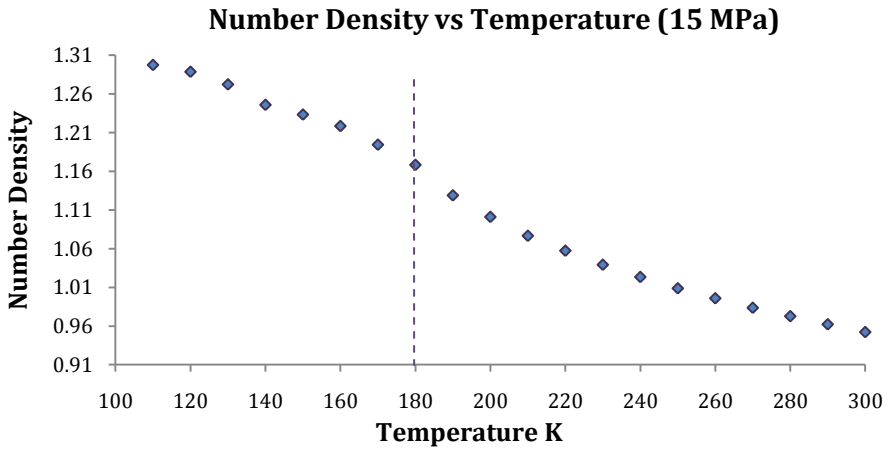

Figure 27: Gives the number density (total number of CO_2 molecules + polymer segments per volume) in the CO_2-polymer box. From the 2-box cooling simulation, using the new CO_2 parameters run at 15 MPa

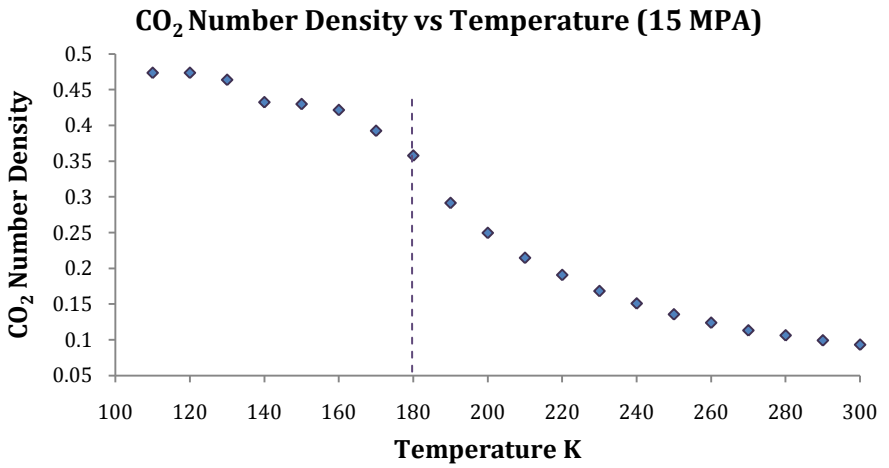

Figure 28: Gives the CO_2 number density (number of CO_2 molecules per volume) in the CO_2-polymer box. From the 2-box cooling simulation, using the new CO_2 parameters run at 15 MPa

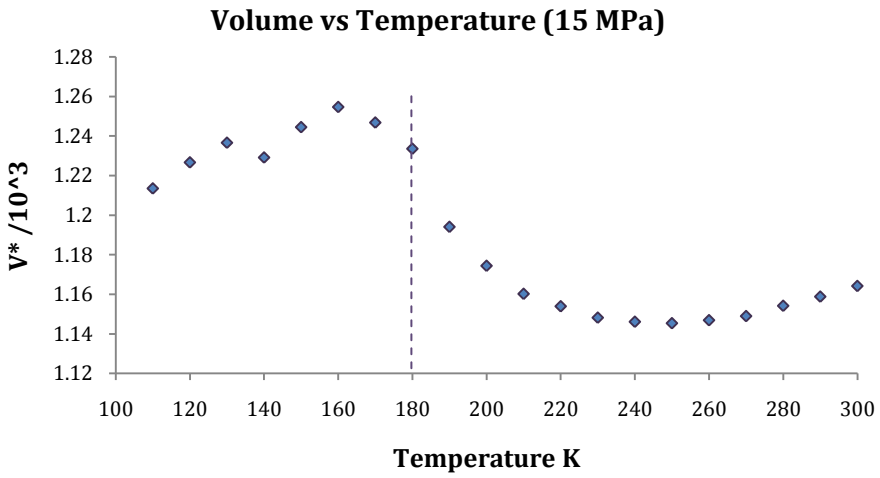

Figure 29: Gives the volume of the CO_2-polymer box. From the 2-box cooling simulation, using the new CO_2 parameters run at 15 MPa

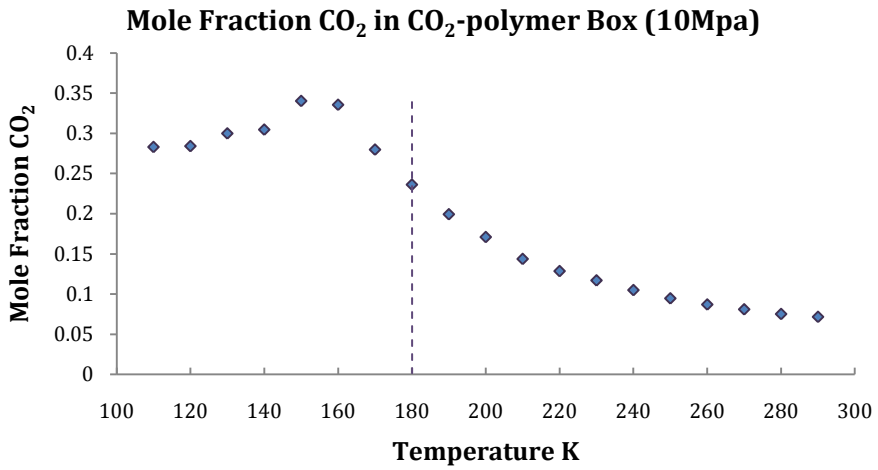

Figure 30: Gives the mole fraction of CO_2 in the CO_2-polymer box. From the 2-box cooling simulation, using the new CO_2 parameters run at 10

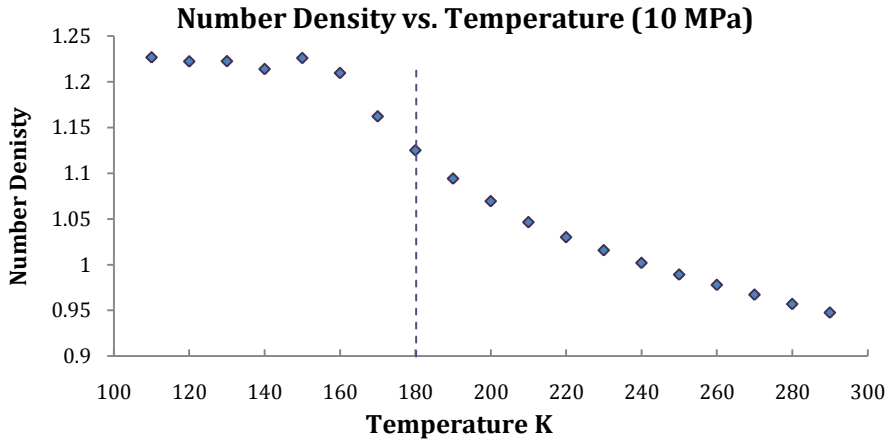

Figure 31: Gives the number density (total number of CO_2 molecules + polymer segments per volume) in the CO_2-polymer box. From the 2-box cooling simulation, using the new CO_2 parameters run at 10 MPa

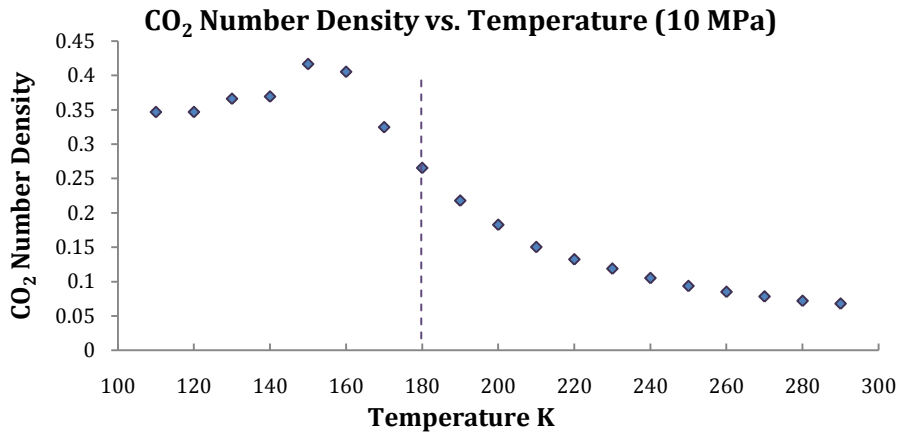

Figure 32: Gives the CO_2 number density (number of CO_2 molecules per volume) in the CO_2-polymer box. From the 2-box cooling simulation, using the new CO_2 parameters run at 10 MPa

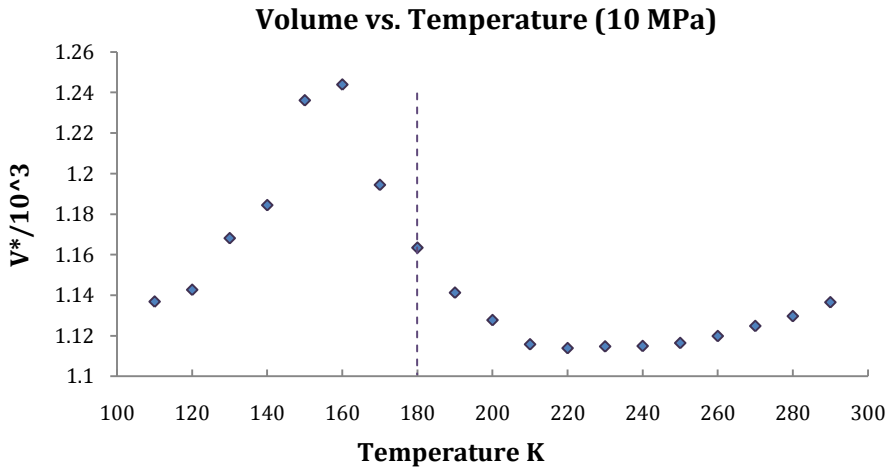

Figure 33: Gives the volume of the CO_2-polymer box. From the 2-box cooling simulation, using the new CO_2 parameters run at 10 MPa

In these graphs a line is added at 180 K [the approximate Glass Transition Temperature of the pure polymer at these pressures] as a visual reference. These graphs are constructed in the hope that trend changes will indicate the glass transition temperature region of the polymer subject to supercritical CO_2. However, a glass transition is not the only possible cause of the observed trend changes. Changes in the pure CO_2 density [number density in the CO_2 box] may also be precipitating a trend change. To explore this possibility, the density of the pure CO_2 is graphed vs. temperature.

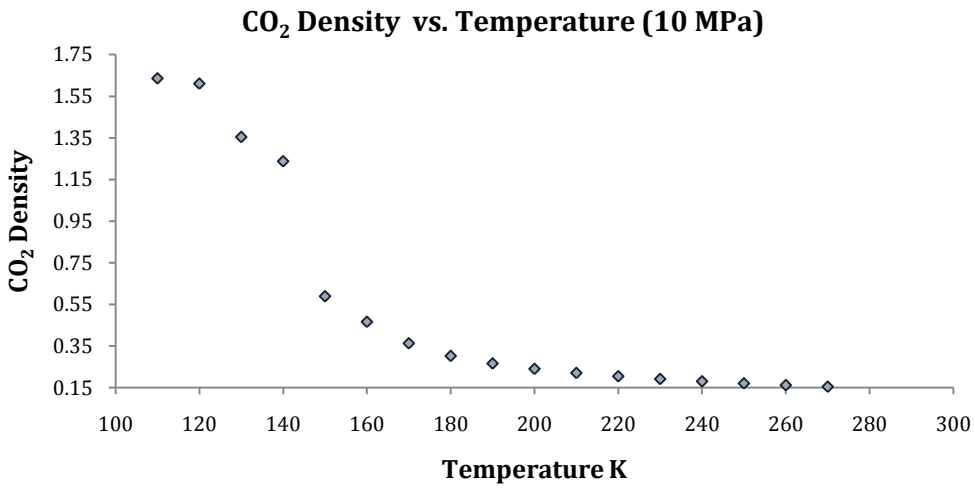

Figure 34: Shows the CO_2 density in the CO_2 only box at 10 MPa.

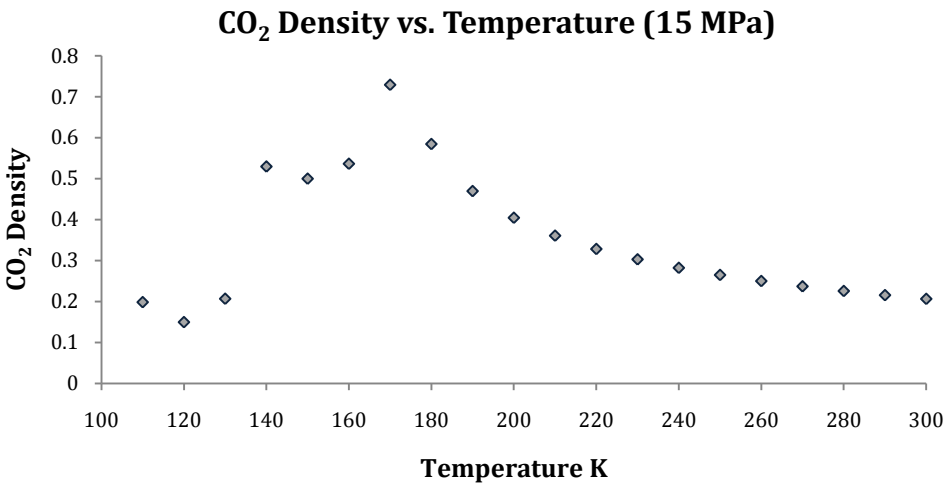

Figure 35: Shows the CO_2 density in the CO_2 only box at 15 MPa. Notice the odd densities for temperatures lower than 180 K

Lacking an explanation for this second graph, the calculated pressure of the pure CO_2 box was examined [although the pressure is set in these simulations it is also independently calculated]. Figure 36 gives the calculated pressure in the pure CO_2 box for simulations run at 15 MPa (P* = .1507461).

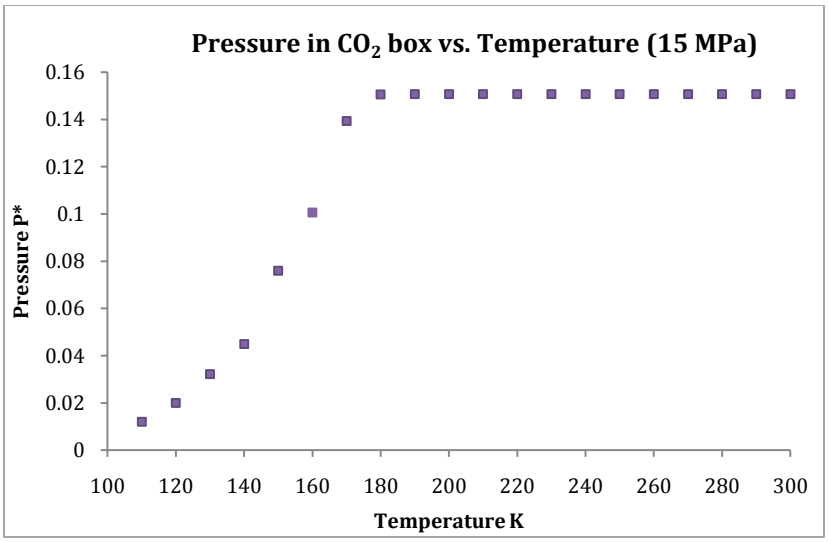

Figure 36: Shows the pressure in the pure CO_2 box (P* that corresponds to 15 MPa is .1507461)

This graph further indicates weird behavior in the region below 180 K. The calculated pressure in the CO_2 box for the simulation run at 10 MPa was also examined, again displaying odd and un-expected behavior (Figure 37).

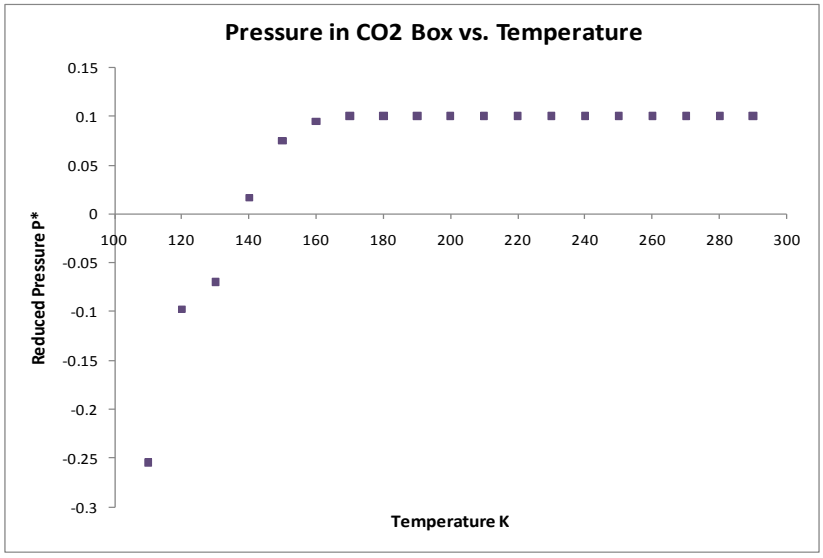

Figure 37: Shows the pressure in the pure CO_2 box (P* that corresponds to 10 MPa is .1004974)

It turns out these results were caused by a computational restriction that did not represent a physical restriction. As mentioned, in order to implement periodic

boundary conditions, the box length must be larger than the interaction cut off distance. As a result there is a lower bound on the size of the simulation box.

Lower Bound on Simulation Box Size

Temperature, pressure and the number of particles determine the equilibrated box volume; however, at the conditions where odd pressures were observed [low simulation temperatures and high simulation pressures] the CO_2 molecules in the CO_2 box would, if not restricted, occupy a volume less than the lower bound.

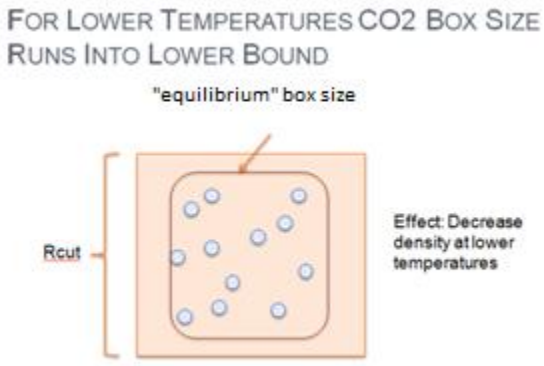

Figure 38: Cartoon depicting the effect of the box size restriction

This issue was circumvented somewhat inelegantly, simply adding CO_2 molecules to the gas-phase box. The number of CO_2 molecules required was also determined in a rough manner, adding molecules until the equilibrated volume was well above the minimum volume required in simulation. The following graphs display the density (Figure 39 and Figure 41) and pressure (Figure 40 and Figure 42) after increasing the number of CO_2 molecules originally placed in the CO_2 box.

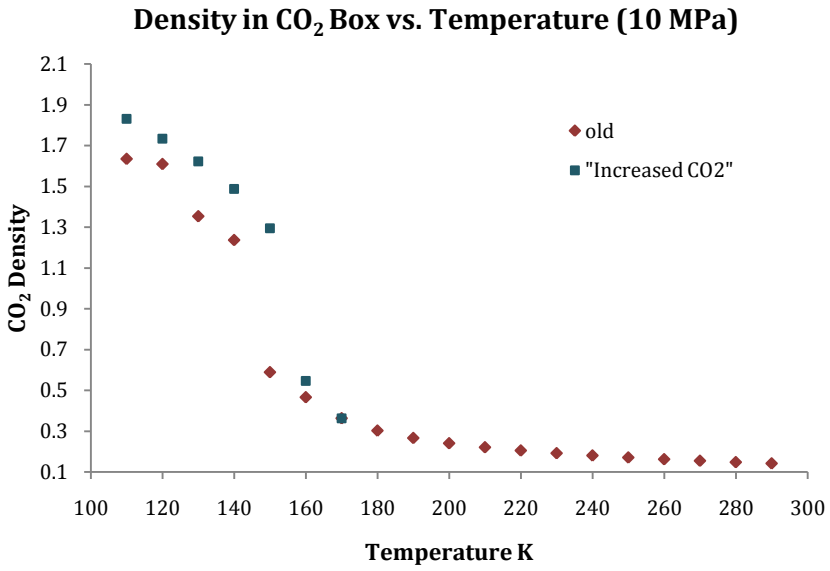

Figure 39: Shows the number density in the CO_2-only box after increasing the number of CO_2 molecules to avoid being restricted by the lower volume bound

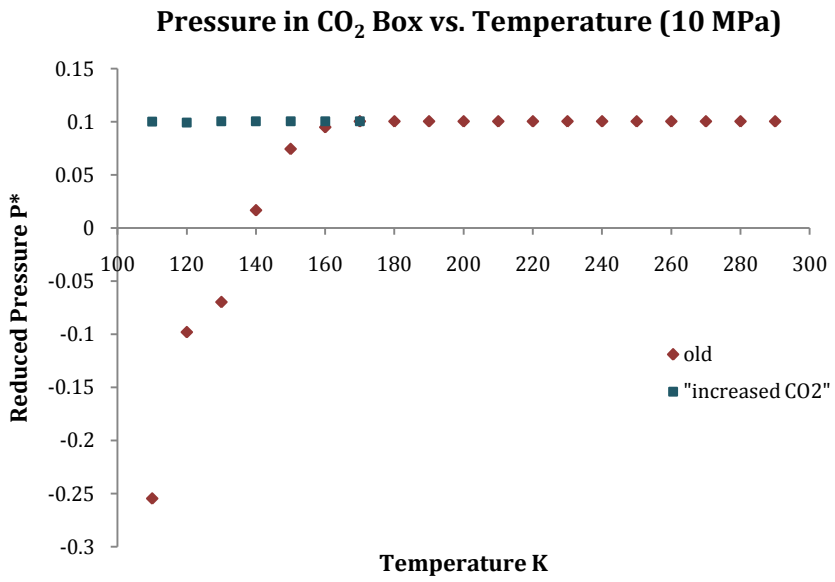

Figure 40: Shows the calculated pressure in the CO_2-only box after increasing the number of CO_2 molecules to avoid being restricted by the lower volume bound

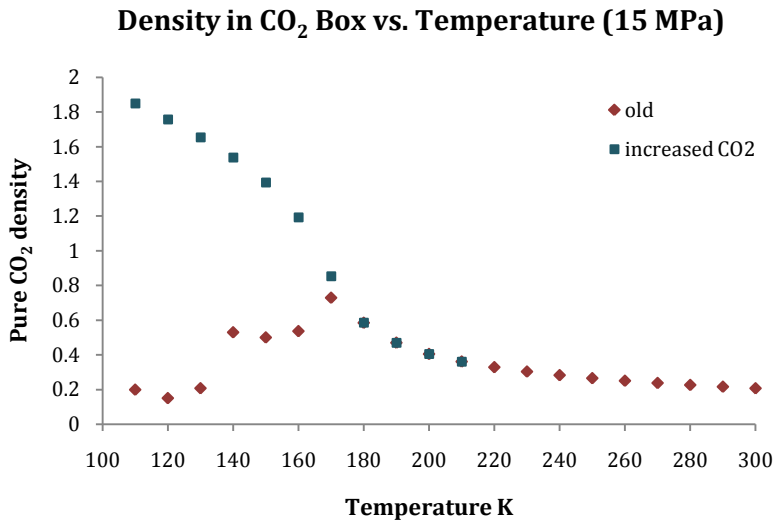

Figure 41: Shows the number density in the CO_2-only box after increasing the number of CO_2 molecules to avoid being restricted by the lower volume bound

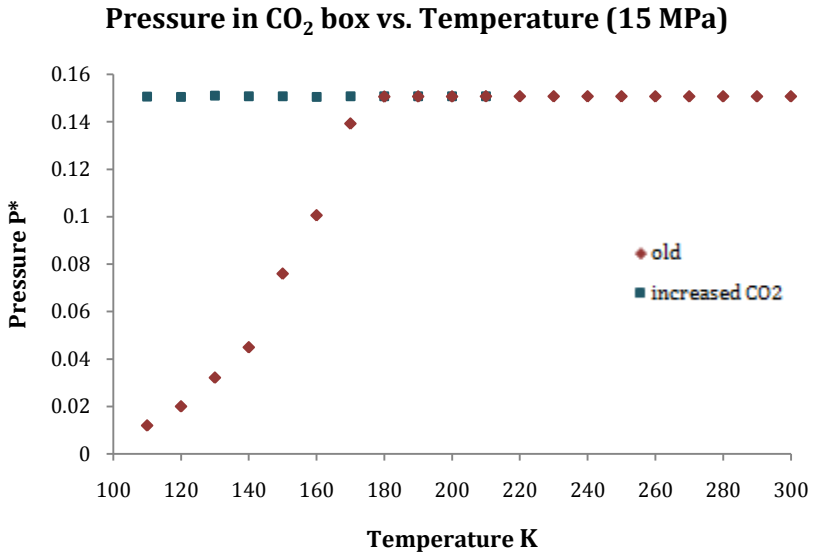

Figure 42: Shows the calculated pressure in the CO_2-only box after increasing the number of CO_2 molecules to avoid being restricted by the lower volume bound

As shown, increasing the number of CO_2 molecules had the desired effect and the calculated pressures are now equal to the set pressure. Also, notice, as might have been expected, that this changes the CO_2 number density and therefore should

affect the amount of CO_2 dissolved in the CO_2-polymer box. Therefore, the characteristics of the CO_2-polymer box were re-examined.

Re-Examination of the Effect of CO_2 on the Polymer Glass Transition Temperature

The following graphs [Figure 43Figure 50] show the mole fraction of CO_2, the overall number density, the CO_2 number density and the volume of the CO_2-polymer box vs. temperature at 10 and 15 MPa [for simulations run after the number of CO_2 molecules placed in the gas box was increased].

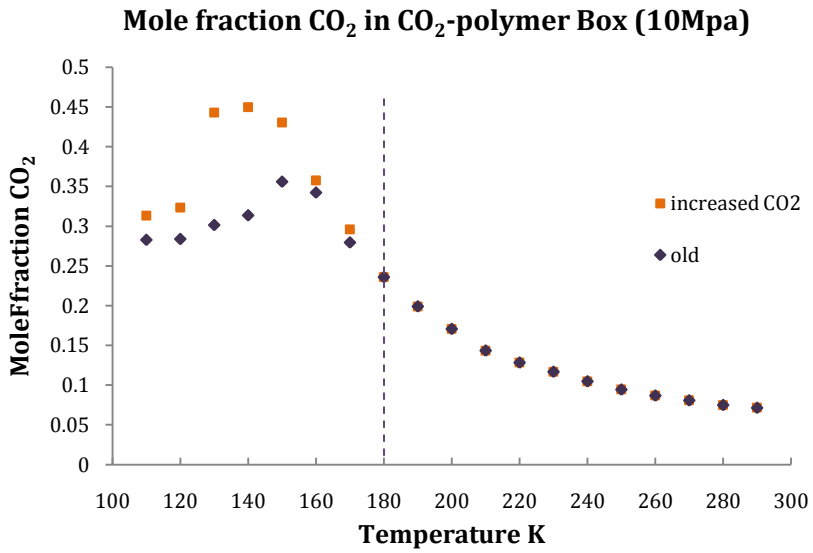

Figure 43: Gives the mole fraction of CO_2 in the CO_2-polymer box. From the 2-box cooling simulation, using the new CO_2 parameters run at 10 MPa

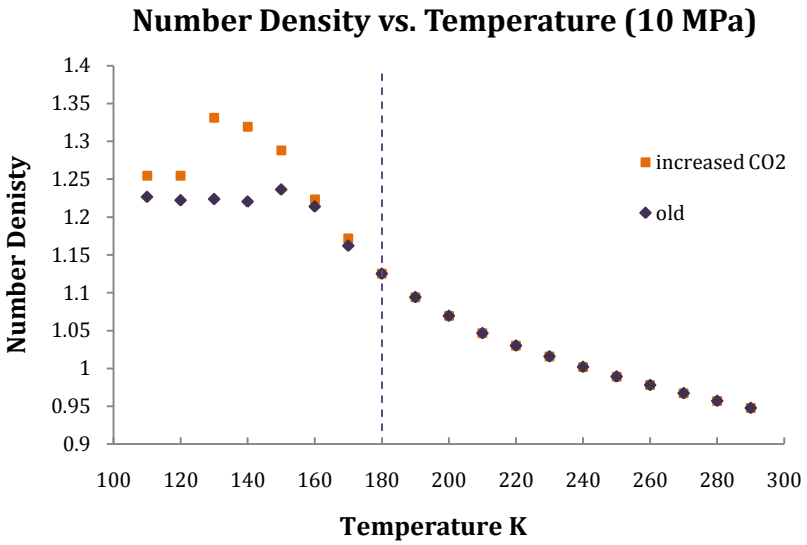

Figure 44: Gives the number density (total number of CO_2 molecules + polymer segments per volume) in the CO_2-polymer box. From the 2-box cooling simulation, using the new CO_2 parameters run at 10 MPa

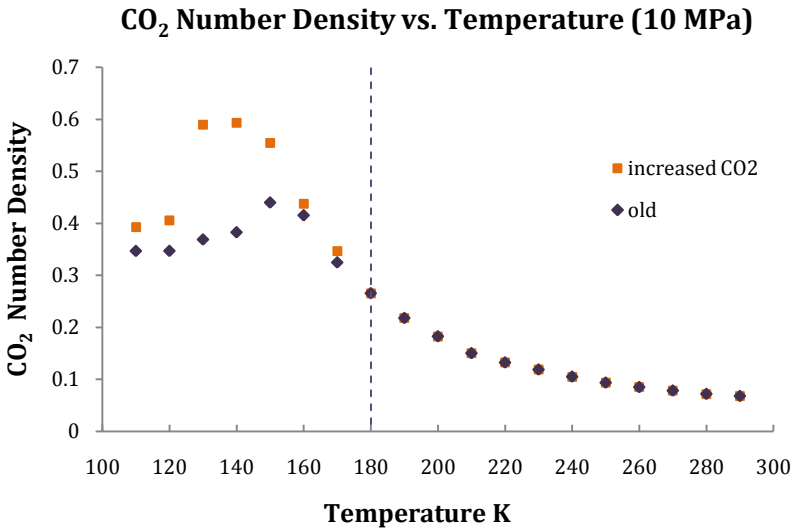

Figure 45: Gives the CO_2 number density (number of CO_2 molecules per volume) in the CO_2-polymer box. From the 2-box cooling simulation, using the new CO_2 parameters run at 10 MPa

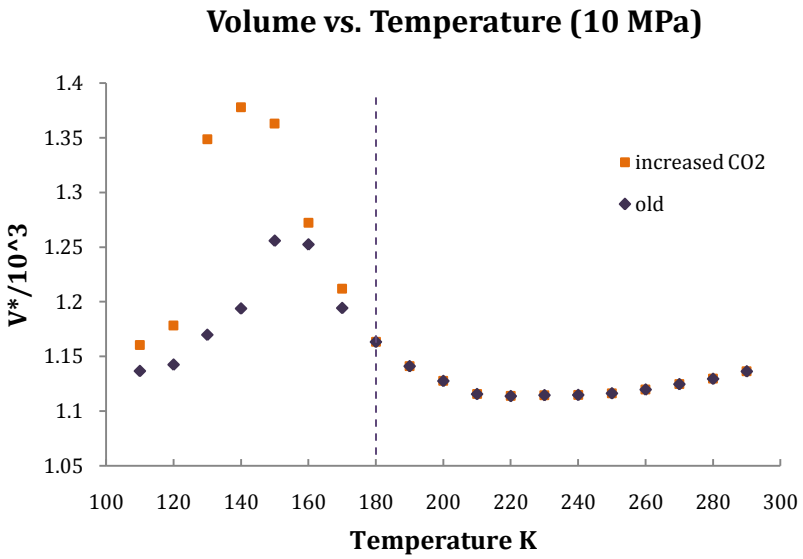

Figure 46: Gives the volume of the CO_2-polymer box. From the 2-box cooling simulation, using the new CO_2 parameters run at 10 MPa

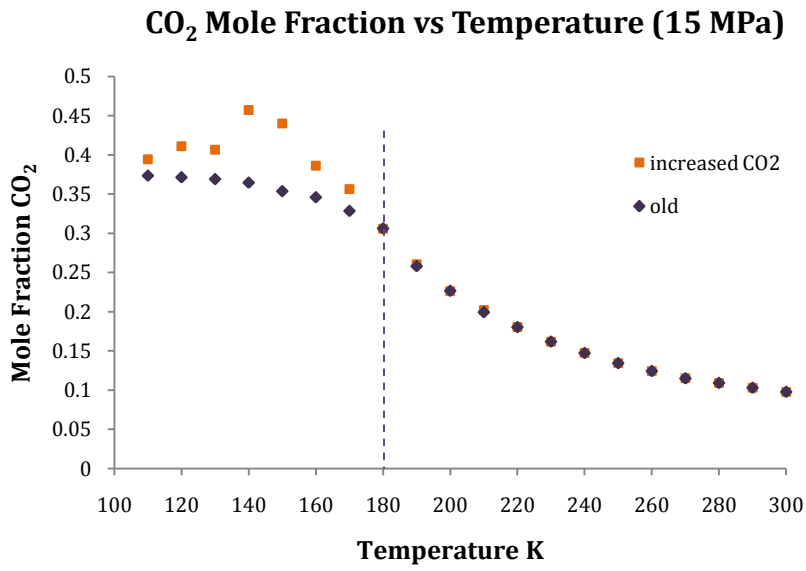

Figure 47: Gives the mole fraction of CO_2 in the CO_2-polymer box. From the 2-box cooling simulation, using the new CO_2 parameters run at 15 MPa

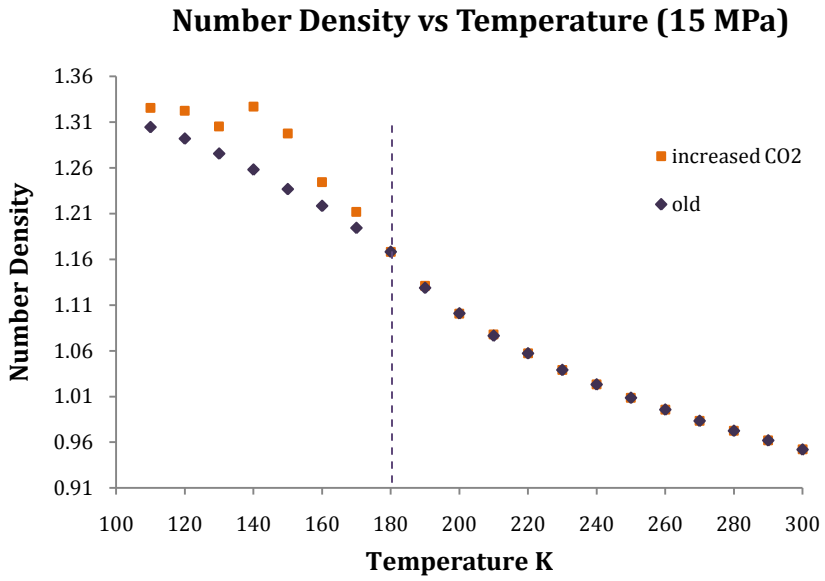

Figure 48: Gives the number density (total number of CO_2 molecules + polymer segments per volume) in the CO_2-polymer box. From the 2-box cooling simulation, using the new CO_2 parameters run at 15 MPa

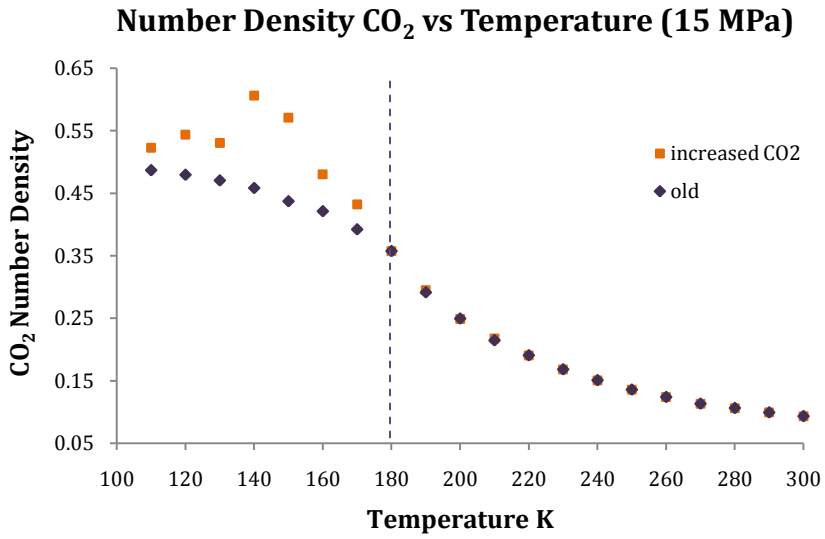

Figure 49: Gives the CO_2 number density (number of CO_2 molecules per volume) in the CO_2-polymer box. From the 2-box cooling simulation, using the new CO_2 parameters run at 15 MPa

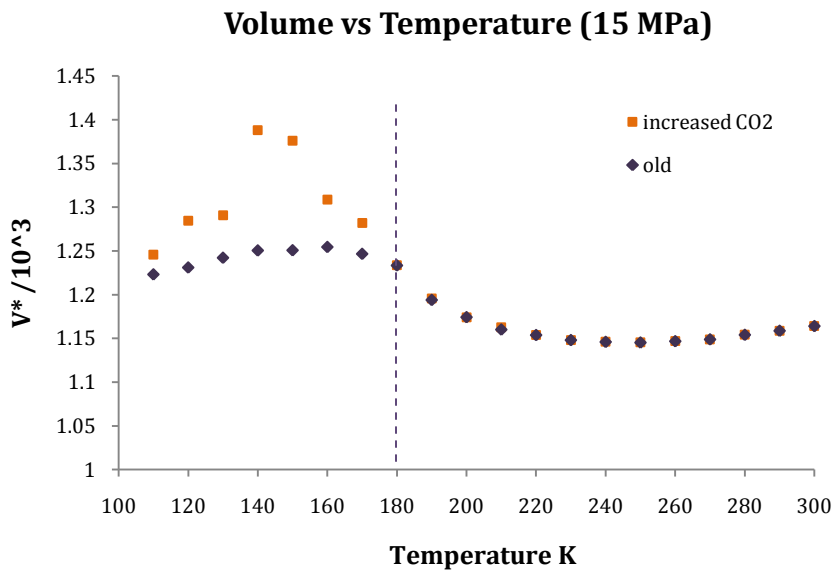

Figure 50: Gives the volume of the CO_2-polymer box. From the 2-box cooling simulation, using the new CO_2 parameters run at 15 MPa

Again, a line is drawn at 180 K as a reference to the Glass Transition Temperature of the pure polymer. Upon examination there does appear to be a fairly consistent trend change at temperatures just below the pure polymer T_g. However, it isn't really satisfactory to just attribute any trend changes to the polymer transitioning from liquid to glass.

The observed trends may be explained in the following way, beginning with the mole fraction of CO_2 in the CO_2-polymer box. At higher temperatures the solubility of CO_2 is low; however, as temperature is decreased more CO_2 is expected to dissolve in the polymer. At approximately 150K a change in the trend of increasing x_{CO2} is observed and, for temperatures lower than 140K, the amount of CO_2 dissolved in the polymer decreases. A possible explanation for this change is glass transition, during which the increasing rigidity of the polymer inhibits more CO_2 molecules from dissolving in the polymer. Next, examining the number density of the CO_2-polymer mixture, one would expect for a fixed number of CO_2 molecules something like the following

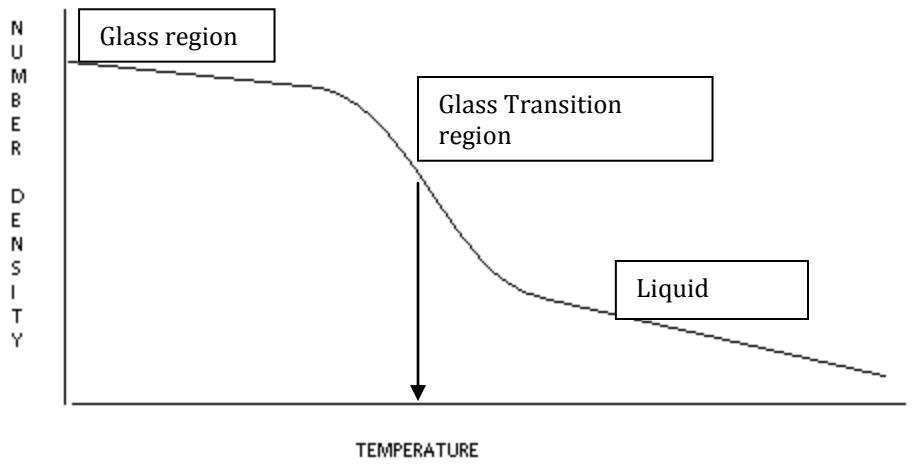

Figure 51: Qualitative sketch of number density vs. temperature for a fixed number of CO_2 molecules in the CO_2-polymer box

In which the density of the mixture changes more with temperature in the liquid region than in the glass region and a large jump in density is observed as the polymer transitions from liquid to glass. This expected trend is somewhat complicated by the fact that the amount of CO_2 in the mixture is not constant – making the regions less distinguishable. The same may be said for the plot of CO_2 number density vs. temperature. Finally, examining the plot of volume vs. temperature, there are a few apparent trend changes. At high temperatures, reducing the temperature reduces the volume of the CO_2-polymer mixture. At about 240K the volume begins to increase with decreasing temperature, this is likely the result of an increasing amount of dissolved CO_2. The volume continues to increase with decreasing temperature until about 140K, at which point it begins to decline with decreasing temperature. A possible explanation of this second trend change is polymer glass transition. That is, due to the onset of the polymer glass transition, CO_2 solubility is inhibited and the amount of dissolved CO_2 no longer increases – because the number of molecules in the CO_2-polymer box is no longer increasing, the volume decreases with decreasing temperature, as expected. Still, it is difficult to confidently attribute the aforementioned trend changes to the glass transition of the simulated polymer. Furthermore, even if we can attribute these trend changes to glass transition, there is no obvious way to extract the exact transition temperature

range. In light of this, the T_g of a polymer subject to CO_2 should be probed in a different manner.

6. Diffusion Coefficient and Glass Transition Temperature

Although the configuration is irregular in a glassy state [as opposed to lattice arrangements observed in many solid states] molecules are never the less constrained to a localized area, and large-scale molecular motion does not take place. The *diffusion coefficient* (D_{MC}) as presented here is indicative of the mobility of polymer segments. This being the case, a polymer in its rigid, glassy state will have inhibited mobility resulting in a D_{MC} near zero. The Glass Transition Temperature should then become obvious when D_{MC} is plotted vs. temperature.

D_{MC} may be found through the observation of the mean squared displacement (MSD) of the polymer segments and is derived in the following way:

$$\gamma = \frac{1}{2t} < (A(t_0+t) - A(t_0))^2 >$$
$$\approx \frac{1}{2}\frac{d}{dt} < (A(t_0+t) - A(t_0))^2 >$$

Where γ represents a general transport coefficient and A represents a general dynamic variable.

Specifically for a constant associated with the rate of displacement, this relationship is the following [for displacement in a single direction]:

$$D \approx \frac{1}{2}\frac{d}{dt} < (x(t_0 + t) - x(t_0))^2 >$$

This can be extended to displacement in any direction with the following:

Equation 7

$$D \approx \frac{1}{6}\frac{d}{dt}\sum_{i=1}^{3} < (x_i(t_0 + t) - x_i(t_0))^2 >$$

The subscript denotes the direction of the displacement, i.e. the y-direction displacement is denoted by x_2.

It should be noted that the *diffusion coefficient* (D) given here is different from what is traditionally called the Diffusion Coefficient, which relates the flux of a species to the concentration gradient or chemical potential gradient.

Although in a MC simulation the system evolves with each Monte Carlo move, rather than in time, we can still obtain a pseudo diffusion coefficient, which serves to indicate the polymer mobility and may indentify the T_g when plotted against temperature. This constant, which has been denoted D_{MC}, is the following:

Equation 8

$$D_{MC} = \frac{1}{6n}\frac{d}{dMC}\sum_{j=1}^{n}\sum_{i=1}^{3}(x_{ji}(MC_0 + MC) - x_{ji}(MC_0))^2$$

Where n represents the number of particles and MC denotes the number of Monte Carlo moves.

Finding the Diffusion Coefficient from a MC CS

As the particle positioning in the simulation box evolves, the MSD is recorded. To obtain $\frac{d}{dMC}(MSD)$ and ultimately D_{MC} a best fit line is applied to the graph of MSD vs. number of Monte Carlo moves – dividing the slope of the best fit line by 6 gives D_{MC}, as shown in the previous section. An example of the MSD vs. Monte Carlo Moves is shown in Figure 52.

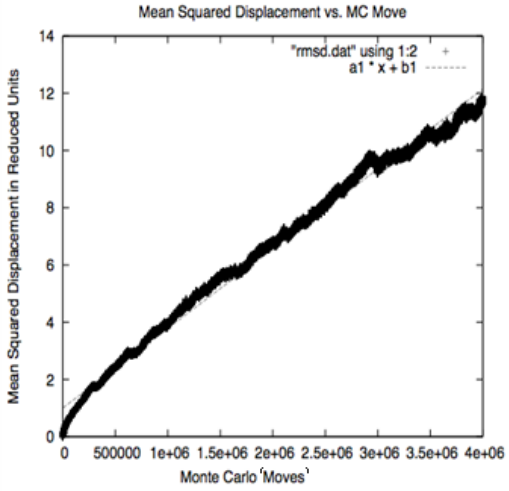

Figure 52: Mean squared displacement including the initial transient portion

Initially, the slope is not constant. This transient portion may be attributed to the uninhibited initial movements [movements away from the initial placement before each molecule contacts or is restricted by the surrounding molecules]. Also, as you can see and as is illustrated more clearly below (Figure 53), including these data points skews the calculated steady-state slope and thus the diffusion calculation [reference Equation 8].

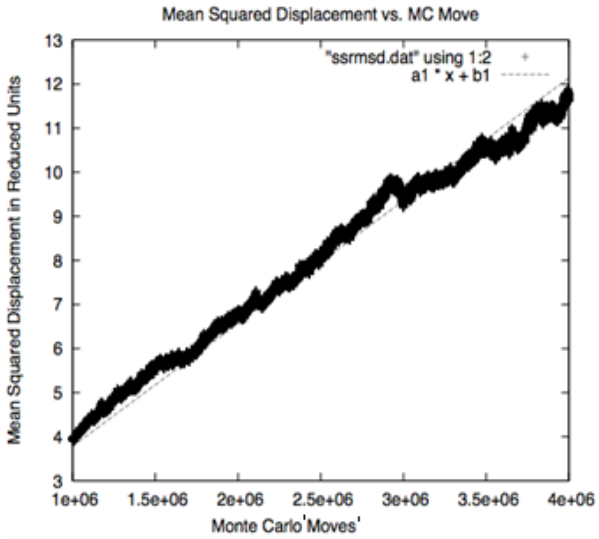

Figure 53: Shows the linear line fit to the *entire* data set in the steady-state diffusion region. Illustrating the error introduced by including the initial, transient, diffusion data.

Therefore, the slope taken as indicative of the diffusion constant was that of the steady slope eventually reached. The transient region data points were disregarded in an ad hoc manner, erring on the side of disregarding more points than necessary as the slope after a certain point is assumed to remain constant.

Diffusion Coefficient of the Polymer Subject to CO_2

The Glass Transition Temperature of our polymer should be revealed by a change in the slope of the polymer *diffusion coefficient* (D_{MC}) vs. temperature [Just as a change in slope of volume vs. temperature revealed the T_g of the simulated pure polymer]. As mentioned, D_{MC} is a measure of how rapidly MSD increases as the system evolves with MC moves. For convenience, the slope of MSD vs. MC moves, which is proportional to D_{MC}, is used as the metric of polymer mobility. The following graphs display $6*D_{MC}$ [the slope of MSD vs. MC moves] vs. temperature at 15 MPa (Figure 54) and 5MPa (Figure 55).

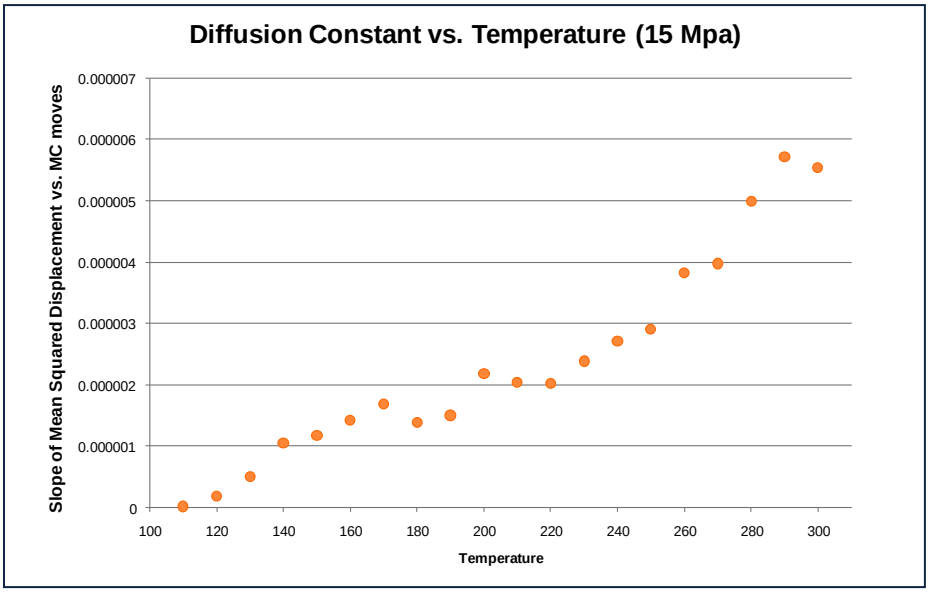

Figure 54: $6*D_{MC}$ vs. temperature for a polymer subject to CO_2 at 15 MPa

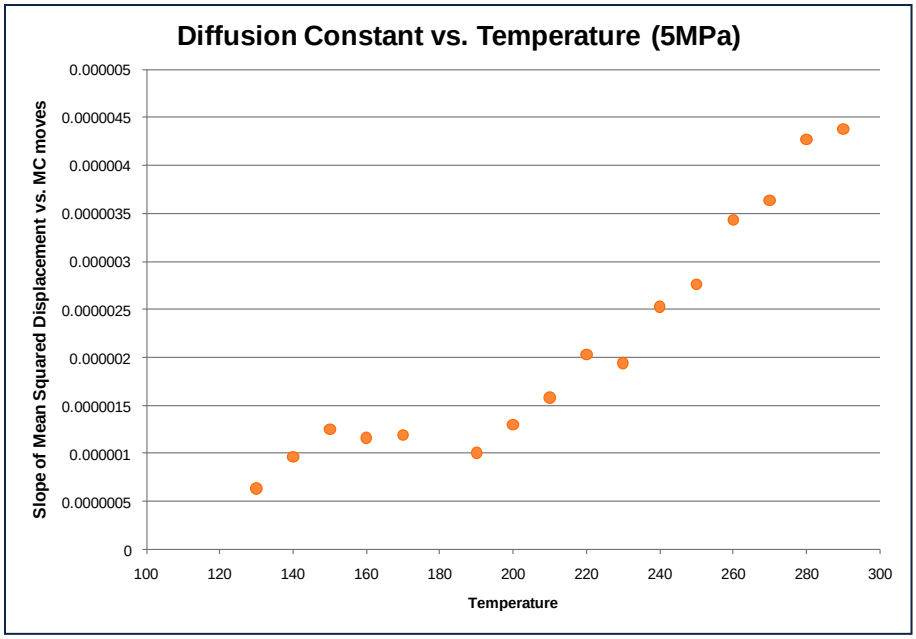

Figure 55: 6*D_{MC} vs. temperature for a polymer subject to CO_2 at 5 MPa. A simulation error resulted in the loss of data at 180K.

These graphs reflect the expected result that the polymer is less mobile at lower temperatures, however, there does not appear to be a clear change in the slope [especially at 15MPa] and it is therefore difficult to identify the T_g from these plots. Furthermore, there is a significant amount of noise. It should be noted that the Asymptotic Standard Error in the best fit line used to obtain the slope of the MSD vs. MC moves is very small [error bars do not extend as far as the size of the plotted dot]. In an attempt average out the noise, the diffusion simulation was replicated. The results are shown in Figure 56 and Figure 57.

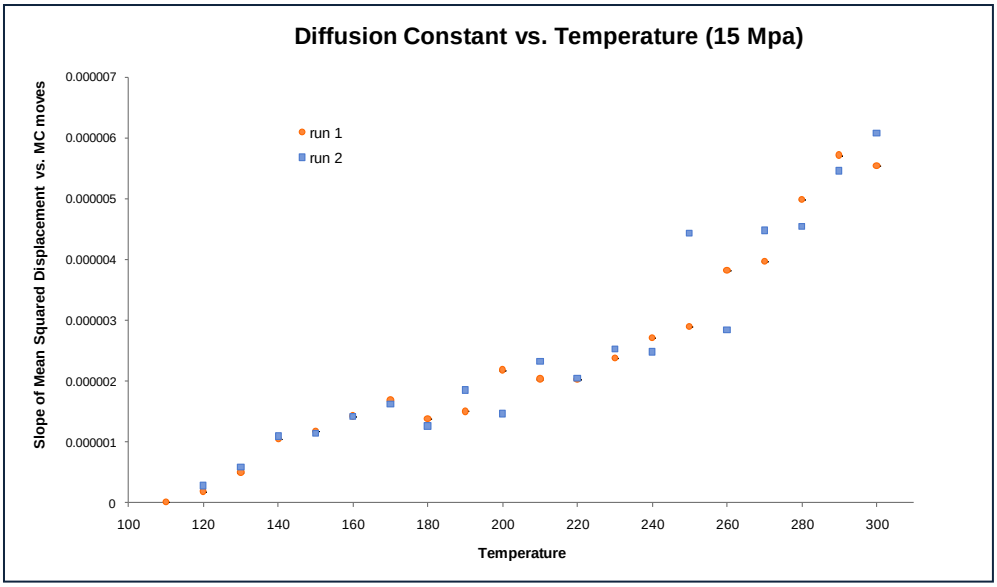

Figure 56: 6*D_{MC} vs. temperature for a polymer subject to CO2 at 15 MPa (both simulations)

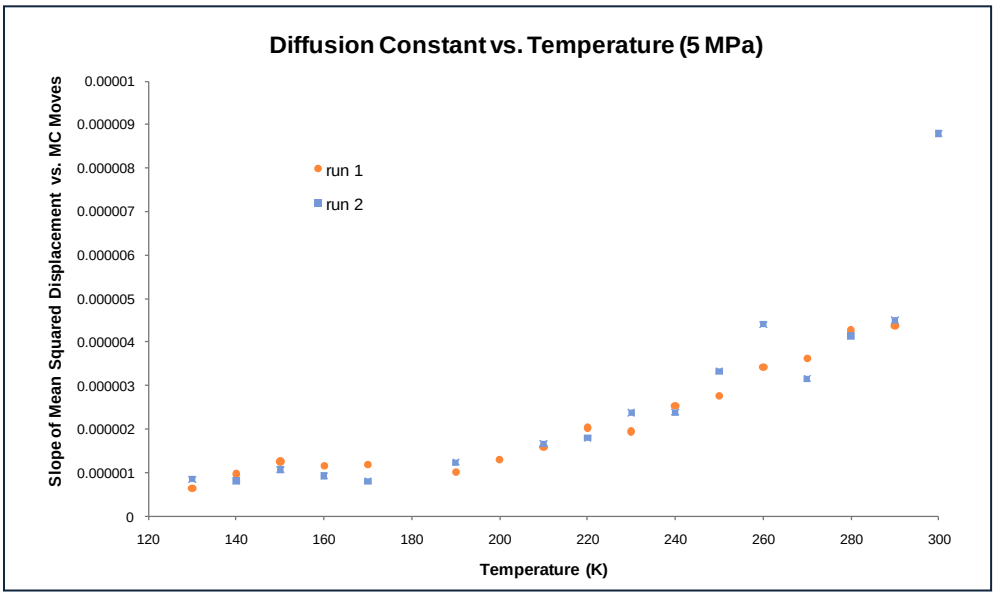

Figure 57: 6*D_{MC} vs. temperature for a polymer subject to CO2 at 5 MPa (both simulations)

From this data, an attempt was made to break the temperatures into three distinct regions, characterized by the slope. Figure 58 and Figure 59 show the categorized data. In Figure 59, the apparent outlier at 300K was omitted.

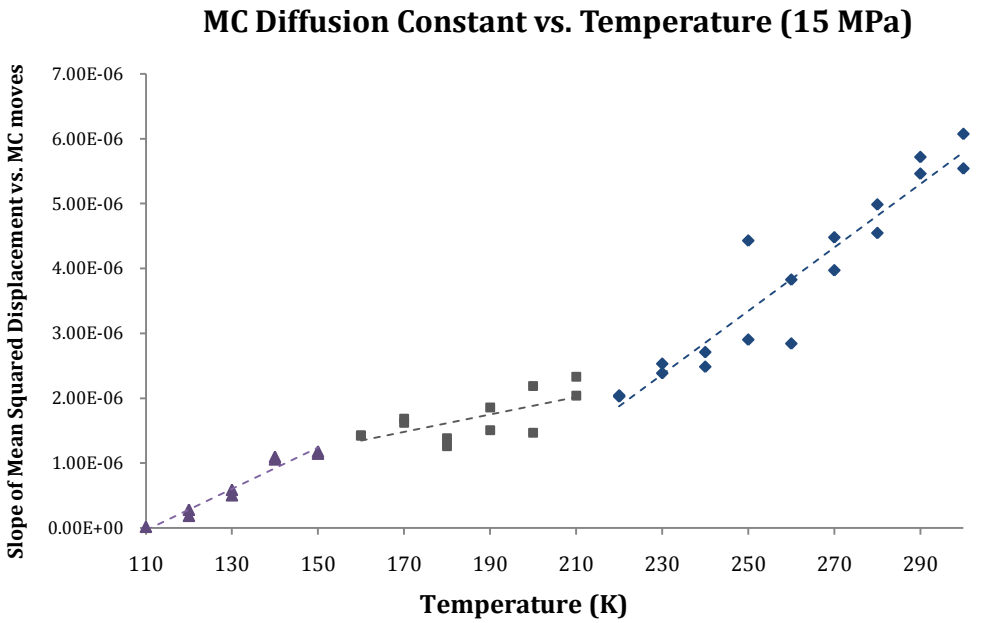

Figure 58: 6*D_{MC} vs. temperature. Data grouped into regions characterized by slope

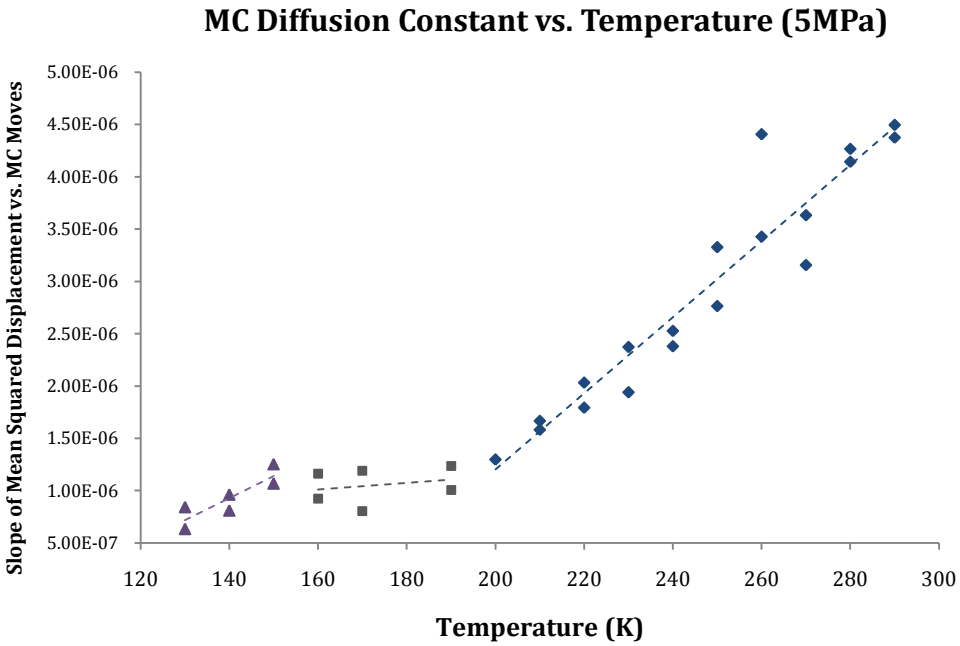

Figure 59: 6*D_{MC} vs. temperature. Data grouped into regions characterized by slope

At both pressures, the slope of the 6*D_{MC} vs. temperature appears to be the smallest in the region the polymer is likely transitioning from liquid to glass. Substantial mobility loss is expected to occur around the glass transition as a result

of the polymer system becoming increasingly rigid, making this result entirely unpredicted.

Pure Polymer Diffusion Coefficient

To explore this unusual behavior, additional simulations were run to obtain diffusion data for the pure polymer. As the glass transition temperature range is known for the pure polymer, the slope changes can be compared to the transition temperatures already found. Figure 60 displays $6*D_{MC}$ vs. temperature for the pure polymer at 15MPa.

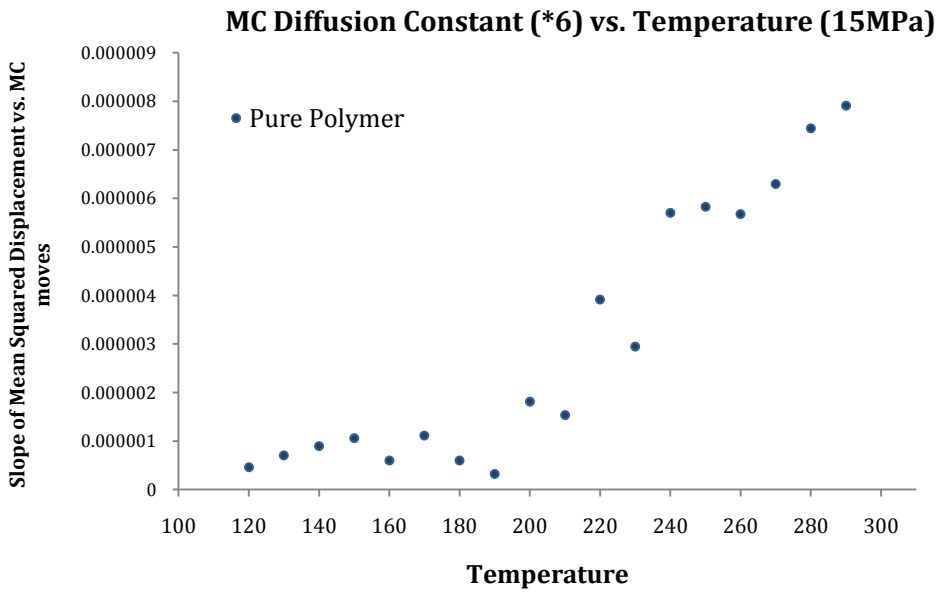

Figure 60: $6*D_{MC}$ vs. temperature for pure polymer at 15 MPa

Previous results allow the above diffusion coefficient data to be categorized into liquid, transition, and glass states accordingly [shown in the next figure, Figure 61].

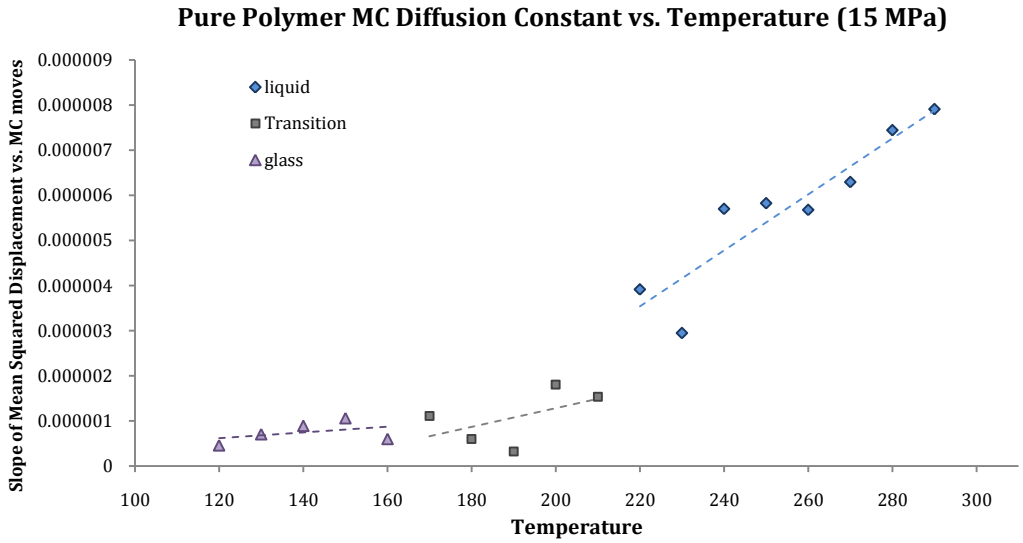

Figure 61: 6*DMC vs. temperature for a pure polymer at 15 MPa. Data categorized as belonging to a liquid, transition, or glassy state per previous cooling simulation on a pure polymer at 15 MPa.

If the glass transition temperature range for the pure polymer at 15MPa was unknown and the sharpest trend changes were used to categorize the data, the pure polymer diffusion data would have been broken up in the following way.

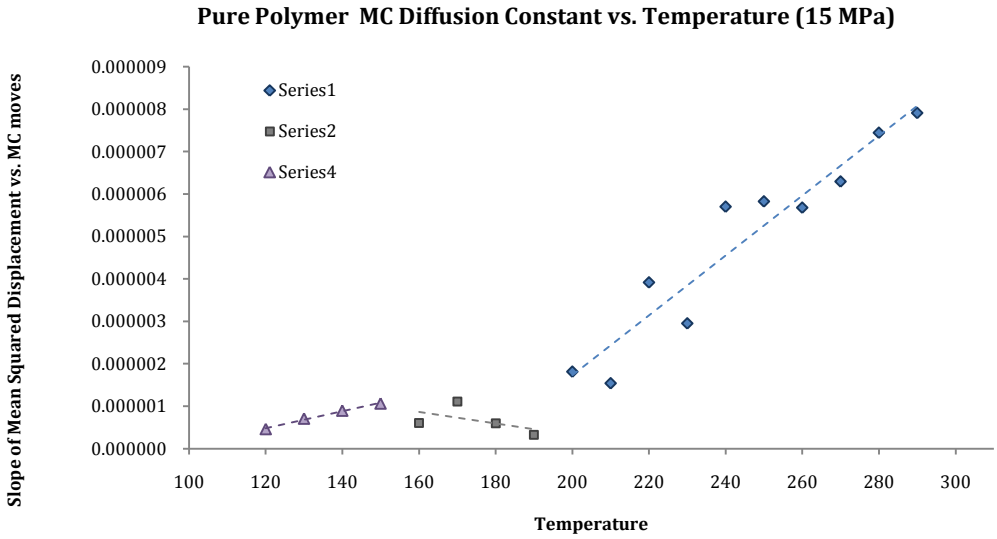

Figure 62: 6*DMC vs. temperature for a pure polymer at 15 MPa. Data split at most apparent trend changes.

As you can see, if these changes in slope were taken to indicate the glass transition range, the glass transition would be assumed to occur from 160-190 K. This is substantially different from the range previously found. However, if the data is broken into two regions – glass and liquid – the break point nearly aligns with the T_g found via the volume vs. temperature plot. This is illustrated in Figure 63.

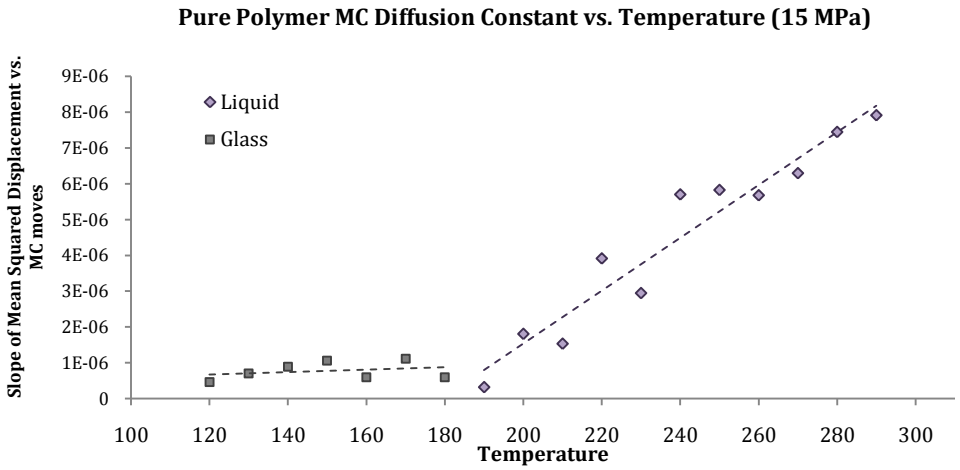

Figure 63: 6*DMC vs. temperature for a pure polymer at 15 MPa. Data broken into two regions, as indicated by a change in slope.

If the same is done for the two-box simulation polymer diffusion data, a break is observed at 173K under 15MPa and around 175K under 5MPa, as shown in Figure 64Figure 65.

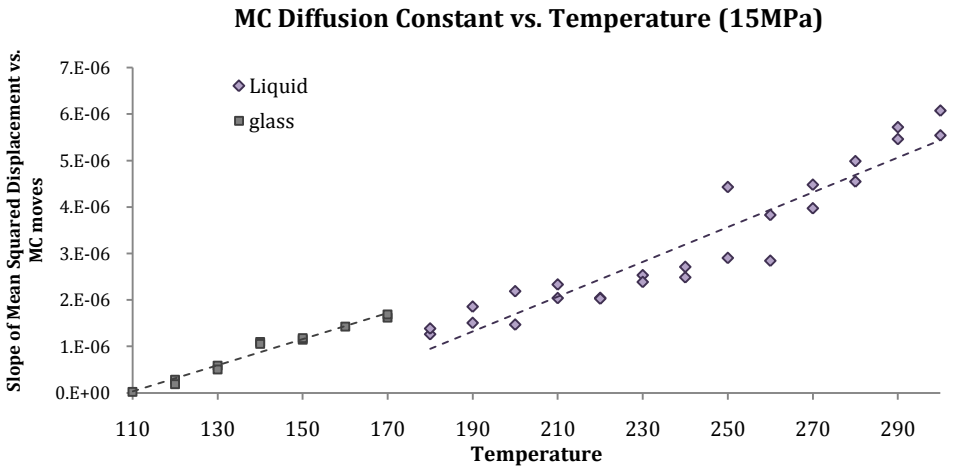

Figure 64: 6*DMC vs. temperature for a pure polymer at 15 MPa. In this graph the data is broken up into just two states characterized by slope.

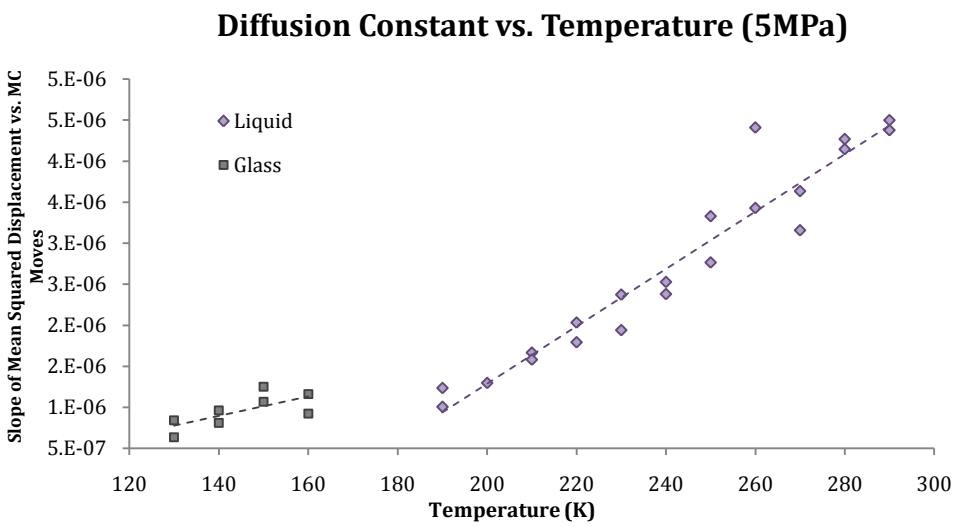

Figure 65: 6*DMC vs. temperature for a pure polymer at 5 MPa. In this graph the data is broken up into just two states characterized by slope. Recall that diffusion data was lost at 180K – this made it difficult to calculate the slope for the surrounding temperatures.

Still, this break is less clear for the CO_2-polymer diffusion data, and as a result it is difficult to confidently claim that the displayed break accurately indicates the glass transition.

7. Work in Progress and Suggested Further Work

Diffusion Coefficient – Further Work

glass region.

In the previous section, the observed *MC diffusion coefficient* [as defined] exhibits odd behavior in the expected glass region. Specifically, it seems odd that D_{MC} is greater than zero and continues to decrease with temperature in low temperature regions where movements should be more or less frozen. It is possible that this is the result of the entire system of molecules drifting in a certain direction, as shifting the whole system would not change the intermolecular potential energy. Although, it seems unlikely that MC molecular rearrangement would result in macro scale drifting, the diffusion of the computer-simulated polymer should be examined at very low temperatures [temperatures where the state may be assumed to be glass]. If diffusion is observed at this temperature, then the computer-simulated polymer is not behaving naturally, and perhaps drifting is taking place during the MC simulation. If this does appear to be the case, polymer diffusion may be re-examined, altering the simulation to restrict system drifting.

revised measure of diffusion.

In the derivation of D_{MC} it was assumed that the state of the system did not evolve over the duration of the simulation. That is to say, it was assumed that diffusion was the result of Brownian motion in a system whose overall [macroscopic properties] remained nearly unchanged. This being the case, the MSD was assumed to increase linearly with MC moves [after what was termed the initial, transient region]. This assumption is relatively easy to check. Consider the following:

Equation 8

$$D_{MC} = \frac{1}{6n}\frac{d}{dMC}\sum_{j=1}^{n}\sum_{i=1}^{3}(x_{ji}(MC_0 + MC) - x_{ji}(MC_0))^2 = \frac{1}{6}\frac{d < (\Delta r)^2 >}{dMC}$$

Integration in steady-state region:

$$D_{MC\ s.s.} * MC = \frac{1}{6} < (\Delta r)^2 >$$

$$\ln(D_{MC\ s.s.}) + \ln(MC) = \ln\left(\frac{1}{6}\right) + \ln(< (\Delta r)^2 >)$$

$$\ln(< (\Delta r)^2 >) = \ln(MC) + c;\ c = \ln(6D_{MC\ s.s.})$$

If the assumption of steady-state linear evolution of MSD is correct, plotting log(MSD) vs. the log(MC) in the assumed steady-state region on a log-log scale should result in a slope of 1.

It turns out, the assumption that the MSD varies linearly after an initial transient period is not entirely accurate. In fact, for 15Mpa the average slope of the log plot described was .74126 and for 5MPa was .74878 (Appendix B displays the results for 15MPa). This suggests that the MSD is actually approximately proportional to $(MC)^{.74}$. Therefore, perhaps a better indicator of mobility can be found fitting the following equation (Equation 9) to the graph of mean squared displacement vs. Monte Carlo moves.

Equation 9

$$< (\Delta r)^2 >= \gamma * [MC]^x$$

$$\gamma \coloneqq mobility\ indicator$$

$$x \coloneqq average\ slope\ found\ via\ the \log plot\ of\ \log(< (\Delta r)^2 >)\ vs. \log(MC\ moves)$$

Volume Deviation

Recall that vitrification occurs when a glass forming substance is cooled sufficiently fast to a sufficiently low temperature, not allowing enough time for rearrangement and relaxation. As a result, a system that exists as a glass exits in an away-from-equilibrium state. The specific molecular configuration and microscopic properties of this system are consequently dependent on path. In other words, the molecular configuration upon freezing will be specific to the cooling process. The uniqueness of each glass configuration, however, does not necessarily show up in observed macroscopic properties. This is likely because, while some small subsystems may have distinctly different properties due to internal stresses etc., the average properties of glasses remain consistent. While this characteristic is not easily observable in experiments, it may provide a way to explore glass transition via *simulation*.

In simulation, we are only simulating a very small amount of molecules or polymers and applying periodic boundary conditions. This being the case, configuration differences in these small systems should be observable. It may therefore be possible to elicit the Glass Transition Temperature by replicating cooling simulations and comparing volume curves.

In the liquid region, volume deviations should be observed, however there should be no clear distinction between the two runs. By this I mean, there should be some noise, but the two curves in the liquid region should not be distinctly different. However, as the system transitions from a liquid to a glass, we should observe two easily distinguishable curves. Replicate two-box cooling simulations were run at 5Mpa the results of which are displayed in Figure 66.

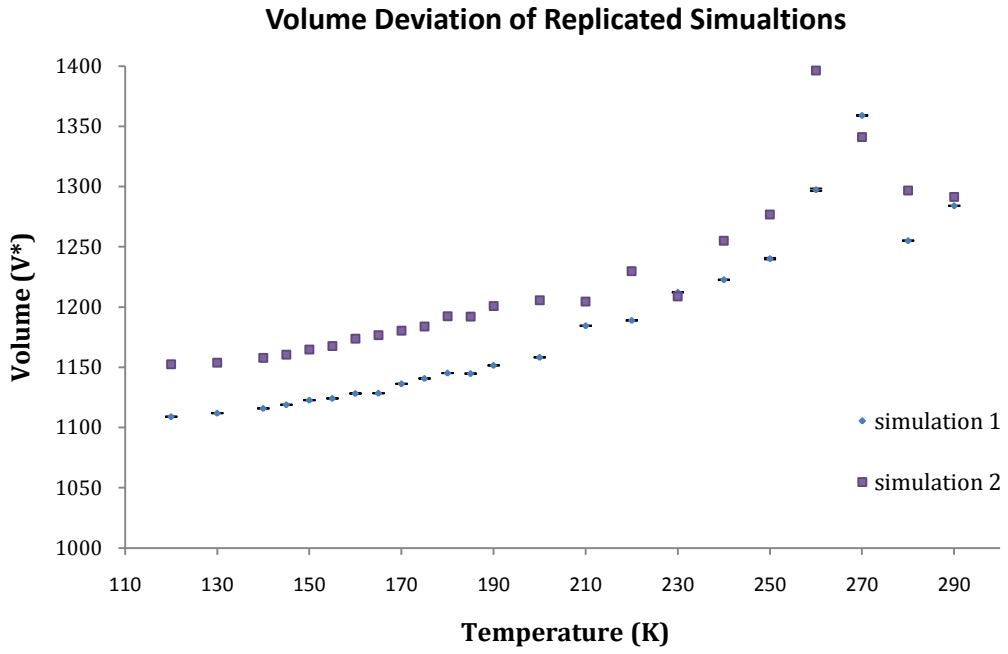

Figure 66: Results of two replicate cooling simulations

From this graph, it appears that two distinctly different curves are observed starting around 200K, perhaps indicating the onset of glass formation. However, as has been the problem with many of these techniques, rigorously identifying the glass transition temperature range from the observed trend is somewhat difficult.

Note that indicating marks for simulation 1 are minimized so that the error bars can be seen. These error bars indicate the volume deviation during the simulation. As shown, the magnitude of the deviation within each simulation is much smaller [the bars aren't even really distinguishable] than the deviation observed between simulations. This illustrates the difficulty in using a MC simulation to simulate the rearrangement of a polymer-CO_2 mixture in contact with gaseous CO_2, as many, many moves are required to obtain the *equilibrium* properties [even in the liquid region]. To more accurately probe the glass transition temperature range using this method, simulations should be allowed to run and equilibrate for an extended period of time [due to time constraints, only short simulation times were used to generate the above data].

Also, note that the general curve is very different from those previously observed. The single difference between the simulation used to generate this data, and the simulations used to generate the previous data is the amount of CO_2 initially placed in the gas-phase box. In previous simulations, the number of CO_2 molecules simulated changed across temperatures in order to avoid simulation box size constraints. This was done under the assumption that the number of CO_2 molecules simulated was irrelevant as long as the CO_2-box volume was allowed to fluctuated and approach the equilibrium volume [this being the case equilibrium pressure and CO_2 density should be entirely independent of the number of molecules in simulation]. However, the uniqueness of the curve generated here brings this assumption into question.

Heating vs. Cooling MC Simulation

The amount of CO_2 dissolved in the polymer and ultimately the Glass Transition Temperature of this polymer may be specific to a cooling process, and therefore subjecting an already cooled rigid polymer structure to CO_2 may result in behavior that is significantly different. To explore this possibility and alleviate this concern, a heating MC CS was undertaken. However, due to time constraints the simulation was not rerun after adding CO_2 to avoid being restricting by the lower volume bound. The results of this initial simulation are given in Appendix C. To address this further, the heating MC CS should be rerun, adjusting the number of CO_2 molecules originally placed in the gas-phase box.

Conclusion

Although interest in nanotechnology is rapidly growing, developing these technologies in the lab invariably requires a clean room and sophisticated equipment; making it very expensive. Furthermore, exploring the phenomena of interest at the scale required is often difficult. Fortunately computer simulation offers an increasingly fast and accurate alternative to many experiments. It was in this context that this research project was undertaken with the goal of developing and using computer simulation to explore the possibility of a CO_2 assisted nanostructure melding process.

This project focused on the use of a Monte Carlo algorithm to simulate the complicated molecular rearrangements that move a system towards equilibrium. The robustness of this algorithm is showcased in its ability to capture the evolution of complicated, multispecies, multiphase systems; however, the utility of this type of simulation largely depends on the development of techniques to probe the properties of interest. Making the use of this medium for nanotechnology research and development [while much cheaper than *lab* experiments] difficult.

As demonstrated, the Glass Transition Temperature of a pure plastic may be found using a MC cooling simulation in which volume is recorded against temperature. Examining the effects of CO_2 on the T_g of that same plastic, however, proves to be more difficult [a non-constant amount of dissolved CO_2 complicates the interpretation of volume changes with temperature]. In light of this, polymer mobility – a characteristic that should reveal the onset of a glass transition – was probed using the pseudo *diffusion coefficient,* D_{MC}. However, a better, more refined metric is required to accurately predict the Glass Transition Temperature. This may be accomplished by extending the same basic concept [rate of change of MSD with MC moves indicates polymer mobility] but relaxing the assumption that MSD is linearly dependent on MC moves and extending the simulation time, reducing the error and noise respectively. Still, even as these methods are refined and the obtained data becomes less nebulous, a gap remains in the ability of simulation to

fully explore the aforementioned melding process. In order to truly examine this process, techniques that probe the interfacial region and simulate polymer-polymer melding must be established.

In the end, this project has been an incremental step towards developing techniques to fully examine the effects of CO_2 on the T_g of plastic nanostructures via Monte Carlo computer simulation.

References

Aziz, R. (1993). Interaction energy of argon dimer. *J. Chem. Phys. Vol. 99* .

Berthelot, D. C. (1898). *C. R. Hebd. Seances Acad. Sci.* , 126.

Lorentz, H. A. (1881). *Ann. Phys. (leipzig) 12* , 127.

Poszwa. (2005, October 9). Retrieved August 13, 2010, from wikipedia: http://en.wikipedia.org/wiki/Lennard-Jones_potential

Sandler, S. I. (2006). *Chemical, Biochemical, and Engineering Thermodynamics.* Danvers, MA: John Wiley & Sons, Inc.

Sato, Y., Tagashira, Y., Maruyama, D., Takishima, S., & Masuoka, H. (1998). Fluid Phase Equilibia. 147.

Talreja, M. (2010). *Towards Understanding Interfacial Phenomena in Polymer-CO2 Systemes.*

Yang, Y., Liu, D., Xie, Y., Lee, L. J., & Tomasko, D. L. (2007). *Advanced Materials 19* , 251.

APPENDICES

Appendix A

statistical analysis.

To describe the reduced volume vs. temperature curve obtained for the pure polymer at 15MPa, the originally discussed mathematical model was proposed.

$$V = \mu + \tau_i + \beta_0 T + (\tau\beta_0)_i T + \beta_1 T^2 + \varepsilon \quad ; \varepsilon \sim N(0, \sigma^2)$$

where $_i$ denotes the state

The following is an outline of the statistical analysis used to validate this model:

Response volume

Regression Plot

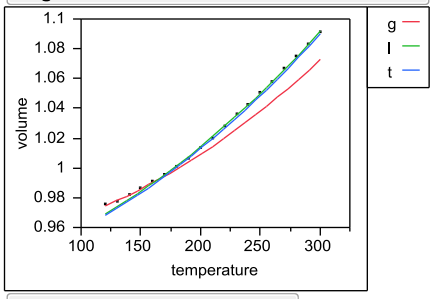

Summary of Fit

RSquare	0.999835
RSquare Adj	0.999752
Root Mean Square Error	0.00059
Mean of Response	1.024966
Observations (or Sum Wgts)	19

Analysis of Variance

Source	DF	Sum of Squares	Mean Square	F Ratio
Model	6	0.02530398	0.004217	12098.62
Error	12	0.00000418	3.486e-7	Prob > F
C. Total	18	0.02530816		<.0001*

Parameter Estimates

Term	Estimate	Std Error	t Ratio	Prob>|t|
Intercept	0.8855153	0.001945	455.36	<.0001*
temperature	0.0006333	1.256e-5	50.44	<.0001*
state[g]	-0.003942	0.001208	-3.26	0.0068*
state[l]	0.0025943	0.000566	4.59	0.0006*
state[g]*(temperature-210)	-8.989e-5	3.915e-5	-2.30	0.0405*
state[l]*(temperature-210)	4.7687e-5	0.000042	1.13	0.2789
(temperature-210)*(temperature-210)	1.1132e-6	3.221e-7	3.46	0.0048*

Effect Tests

Source	Nparm	DF	Sum of Squares	F Ratio	Prob > F
temperature	1	1	0.00088669	2543.729	<.0001*
state	2	2	0.00000737	10.5654	0.0023*
state*temperature	2	2	0.00000475	6.8066	0.0106*
temperature*temperature	1	1	0.00000416	11.9455	0.0048*

Again, this analysis suggests that state does in fact have a statistically significant effect on the slope of volume vs. temperature.

To describe the reduced volume vs. temperature curve obtained for the pure polymer at 10MPa, the same mathematical model was proposed; however, upon statistical analysis it was found that the T^2 contribution was not statistically significant. That is to say, the change of volume with temperature in a given state is not significantly non-linear. The best model in this case is:

$$V = \mu + \tau_i + \beta_0 T + (\tau\beta_0)_i T + \varepsilon \quad ; \varepsilon \sim N(0, \sigma^2)$$

where $_i$ denotes the state

Statistical analysis of the pure polymer V* vs. T at 10 MPa using the above model:

Response Volume

Regression Plot

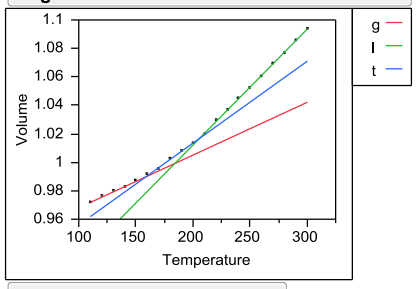

Summary of Fit

RSquare	0.999841
RSquare Adj	0.999784
Root Mean Square Error	0.000573
Mean of Response	1.023826
Observations (or Sum Wgts)	20

Analysis of Variance

Source	DF	Sum of Squares	Mean Square	F Ratio
Model	5	0.02890549	0.005781	17577.61
Error	14	0.00000460	3.289e-7	Prob > F
C. Total	19	0.02891009		<.0001*

Parameter Estimates

Term	Estimate	Std Error	t Ratio	Prob>|t|
Intercept	0.8935334	0.001452	615.44	<.0001*
Temperature	0.0005845	8.804e-6	66.39	<.0001*
State[g]	-0.006162	0.000947	-6.51	<.0001*
State[l]	0.0029291	0.000549	5.33	0.0001*
(Temperature-205)*State[g]	-0.000215	1.368e-5	-15.71	<.0001*
(Temperature-205)*State[l]	0.0002253	9.529e-6	23.65	<.0001*

Effect Tests

Source	Nparm	DF	Sum of Squares	F Ratio	Prob > F
Temperature	1	1	0.00144977	4408.073	<.0001*
State	2	2	0.00001393	21.1778	<.0001*
Temperature*State	2	2	0.00020482	311.3750	<.0001*

While this analysis suggests a different mathematical model, it still indicates that state does in fact effect the rate of change of volume with temperature.

Appendix B

slope of log plot vs. temperature.

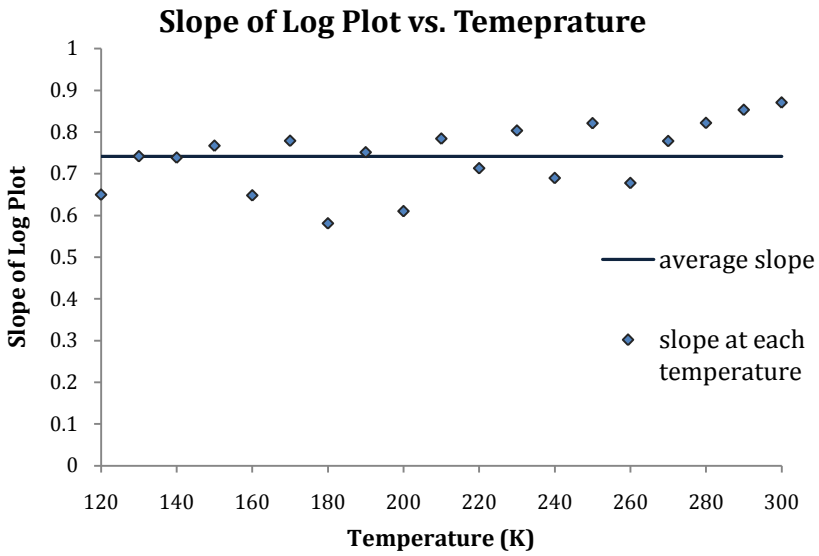

Figure 67: Displays the slope of $\log(< (\Delta r)^2 >)$ $vs.$ **log** $(MC\ moves)$ **against temperature**

Appendix C

cooling vs. heating MC CS.

In this simulation the polymer is allowed to equilibrate at 100 K (well below the T_g of the pure polymer) before CO_2 is introduced. After which a heating process, similar to the cooling process, is implemented. Starting at 100 K and 10 Mpa the polymer subject to CO_2 via a two-box simulation is equilibrated for 20,000 MC steps at which point the configuration is copied and the temperature is raised 10 K. This process is repeated until 300 K is reached. The following graphs give the results of this heating simulation.

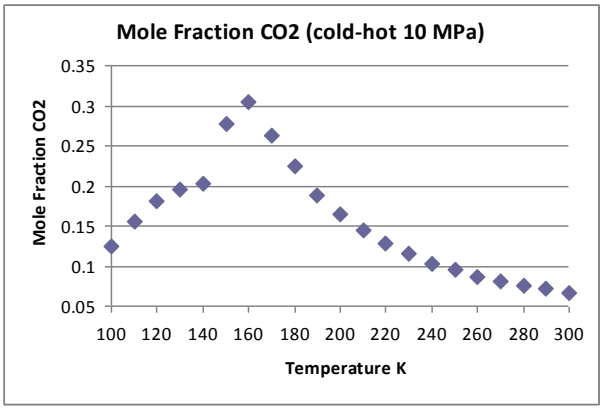

Figure 68: Gives the mole fraction of CO2 in the CO2-polymer box. From the 2-box heating simulation, using the new CO2 parameters run at 10 MPa

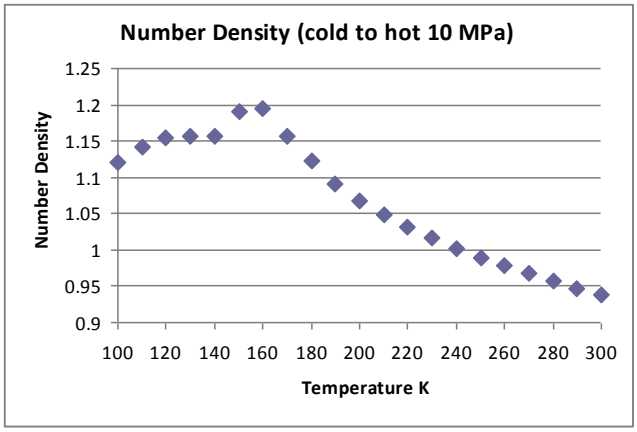

Figure 69: Gives the number density (total number of CO2 molecules + polymer segments per volume) in the CO2-polymer box. From the 2-box heating simulation, using the new CO2 parameters run at 10 MPa

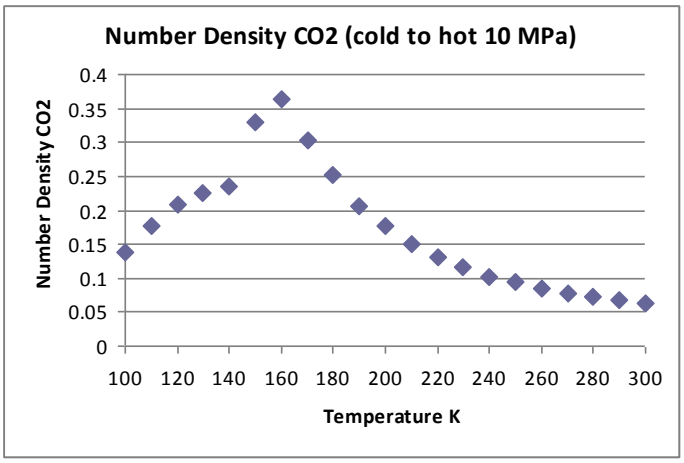

Figure 70: Gives the CO2 number density (number of CO2 molecules per volume) in the CO2-polymer box. From the 2-box heating simulation, using the new CO2 parameters run at 10 MPa

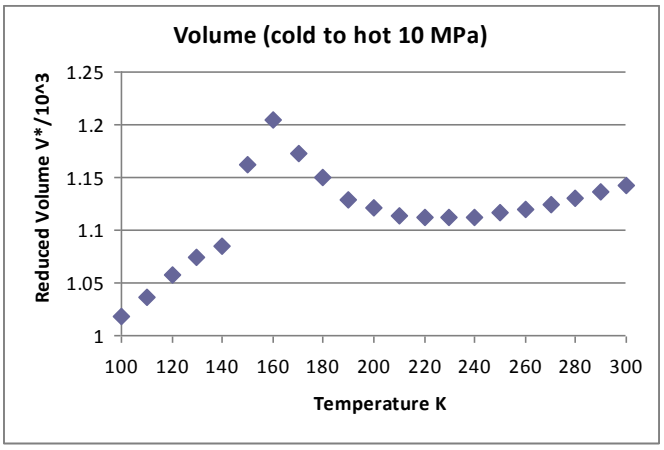

Figure 71: Gives the volume of the CO2-polymer box. From the 2-box heating simulation, using the new CO2 parameters run at 10 MPa

Although, the amount of CO_2 and, consequently, the number density and the volume of the CO_2-polymer box are markedly different [compared to the initial results of the cooling simulation] for temperatures below the proposed Glass Transition Temperature, the temperature at which a clear trend change takes place remains the same. Furthermore, as this temperature is approached, the difference between the amount of dissolved CO_2 observed for the heating process and the amount of dissolved CO_2 observed for cooling diminishes. Therefore, although the amount of dissolved CO_2 at low temperatures appears to depend on the process, the effect CO_2 has on the T_g does not appear to change.